

Modelling primary production: multitude of theories, or multitude of languages?

Jozef Skákala^{1,2}, Shubha Sathyendranath^{1,2}, Yuri Artioli¹, Deep S Banerjee^{1,2}, Heather Bouman³, Robert J.W. Brewin⁴, Momme Butenschön⁵, Stefano Ciavatta⁶, Stephanie Dutkiewicz⁷, Yanna Fidai¹, David Ford⁸, Grinson George⁹, Karen Guihou⁶, Bror Jönsson¹⁰, Marija Bačekočić Koloper¹¹, Žarko Kovač¹¹, Lekshmi Krishnakumary¹, Gemma Kulk^{1,2}, Charlotte Laufkötter¹², Gennadi Lessin¹, Jann Paul Mattern¹³, Angélique Melet⁶, Alexandre Mignot⁶, David Moffat^{1,2}, Fanny Monteiro¹⁴, Mayra Rodriguez Bennadji⁴, Cécile S. Rousseaux¹⁵, Ranjini Swaminathan¹⁶, Osvaldo Ulloa¹⁷ and Jerry Tjiputra¹⁸

¹Plymouth Marine Laboratory, UK,

²National Centre for Earth Observation, UK,

³University of Oxford, UK,

⁴University of Exeter, UK,

⁵Euro-Mediterranean Center on Climate Change (CMCC), Italy,

⁶Mercator Ocean International, France,

⁷Massachusetts Institute of Technology, USA,

⁸Met Office, UK,

⁹Central Marine Fisheries Research Institute, India,

¹⁰University of New Hampshire, USA,

¹¹University of Split, Croatia,

¹²University of Bern, Switzerland,

¹³University of California, Santa Cruz, USA,

¹⁴University of Bristol, UK,

¹⁵National Aeronautics and Space Administration (NASA), USA,

¹⁶University of Reading, UK,

¹⁷University de Concepción, Chile,

¹⁸NORCE Research AS, Norway

Correspondence to: Jozef Skakala (jos@pml.ac.uk)

Abstract. Marine primary production, converting approximately 50Gt of inorganic carbon into organic carbon per year, is an important component of the global carbon cycle, and a major determinant of past, present and future climate. Large-scale, long-term estimates of marine primary production rely primarily on two types of models: satellite-based models that make extensive use of remote-sensing data, and ecosystem models providing numerical simulation of ecological processes embedded in general ocean circulation models. Intercomparison exercises of model outputs (both within and across the two model types) have consistently revealed high discrepancies between estimated global ocean primary production, including divergent magnitudes and even opposite trends. Model-observation comparisons are also complex, because paucity of data, differences in measurement techniques, and evolving methodologies could all lead to difficulties with the interpretation of results. These uncertainties limit the applications of primary production models (both satellite-based and ecosystem), especially in the climate context, where an important question is whether climate change will drive significant future changes in regional or global primary production. Both satellite-based and ecosystem models rely on a range of fixed model parameters, whose values need to be carefully estimated and tested. In this paper, we suggest that such model parameters represent an underappreciated but important source of inter-model differences. With the proliferation

47 of both satellite and *in situ* observations of relevant variables at global scales, and the availability of powerful
48 statistical tools such as data assimilation and machine learning, we argue that time is right to systematically
49 examine model parameters, gaining both better insights into parameter values and how those values might vary
50 in space and time. We argue that such spatio-temporal parameter variability can be theoretically justified for
51 ecosystem models with complexity similar to those commonly used within Earth System Models (ESMs) in
52 climate studies. The spatially and temporally varying parameter values could serve to unify models that are
53 structurally different. An important aspect of this unification could be the ability to infer the spatio-temporal
54 variability of parameters in the less complex models from the emergent behaviour of the more complex ones. This
55 could include ecosystem model simulations of nutrients, temperature, phytoplankton classes, or vertical
56 distributions informing satellite-based models. We conclude that better understanding of model parameter roles
57 and integration (or inter-calibration) of different types of models could reduce discrepancies among the primary
58 production models and improve the reliability of marine primary production projections.

59
60

61 **1. Introduction**

62 The climate problem is highly complex, the stakes are very high, and substantial knowledge gaps remain,
63 especially in the ocean biogeochemistry domain (Kwiatkowski *et al.*, 2020). More broadly, the need to address
64 complex issues related to the carbon cycle, ecosystem services and biogeochemistry through Earth System Models
65 (ESMs), e.g., in the context of climate adaptation and resilience, has been highlighted by expert groups (Hewitt
66 *et al.* 2021). Similarly, Jones *et al.* (2024) evaluate modelling priorities to support international climate policy and
67 emphasise the value of “a coordinated, internally consistent set of simulations, data, and knowledge to support
68 Intergovernmental Panel on Climate Change (IPCC) assessments” and outline multiple applications of Coupled
69 Model Intercomparison Project (CMIP) projections. These include investigations of threats to marine ecosystems
70 (which have consequences for the ocean’s ability to buffer climate change, Tjiputra *et al.*, 2025) and downstream
71 services under various climate scenarios and associated risks of tipping points. Jones *et al.* (2024) also state that
72 improving confidence in future projections requires models to reproduce the observed historical period.
73 Furthermore, they identify parameter uncertainty as one of the key elements of uncertainty in climate models.

74 Against this background and in line with the recommendations of expert bodies, we focus on the climate
75 priority challenge associated with marine ecosystem and biogeochemistry modelling, and particularly on marine
76 primary production. Phytoplankton primary production (PP), the process by which marine autotrophs convert CO₂
77 into organic matter through photosynthesis, is a major component of the ocean and planetary carbon cycle.
78 Currently estimated at around 50 Pg C y⁻¹ (Kulk *et al.* 2020, 2021), the magnitude of marine PP is five times the
79 estimated fossil fuel emissions of 10 Pg C y⁻¹ in 2022 and nearly 20 times the net ocean carbon sink (Friedlingstein
80 *et al.* 2024). Its magnitude is comparable to that of terrestrial primary production (Lurin *et al.* 1994; Longhurst *et al.*
81 1995; Field *et al.* 1998; Friedlingstein *et al.* 2024). A key question in climate research is whether the current
82 levels of marine PP can be maintained under climate change (Tagliabue *et al.*, 2021), when marine ecosystems
83 are increasingly threatened by a variety of processes, including ocean acidification (Jin *et al.*, 2020, Dai *et al.*,
84 2025), rising seawater temperatures (Kwiatkowski *et al.*, 2020), intensified storminess over the oceans (Gastineau
85 and Soden, 2009, Young *et al.*, 2019, Gentile *et al.*, 2023, Liu *et al.*, 2024), ocean deoxygenation (Schmidtko *et al.*
86 *et al.*, 2017), modified current and stratification influencing surface nutrients (Maishal, 2024), changes in aerial
87 nutrient supply (Bergas-Masso *et al.*, 2025), biodiversity loss (Luypaert *et al.*, 2020), and sea-ice loss (Mykswoll

88 *et al.*, 2023). In this review we consider PP estimated from two types of models: “satellite-based models” that
89 utilise remote-sensing data together with physiological models, whose parameters are informed by *in situ*
90 measurements, to calculate PP; and mechanistic “ecosystem models” which use numerical methods to solve a set
91 of differential equations representing many ecological processes, with one of them being PP.

92 When discussing marine PP it is important to keep track of its different components. Theoretically, PP before
93 any of the loss terms are considered is referred to as gross PP (GPP); once the respiration by marine autotrophs is
94 subtracted from GPP we obtain net PP (NPP). GPP can also be partitioned according to whether only the organic
95 carbon fixed into particulate material is considered (production of particulate organic carbon), or if the exudates
96 (dissolved organic matter) are also included in the estimate (production of total organic carbon, Regaudie-de-
97 Gioux *et al.* 2014). Models can make explicit distinction between these components, though this is not always
98 done. *When it comes to in situ observations, experimental methodologies and carefully assembled protocols exist*
99 *for measurement of each of these components (IOCCG, 2022); however, practical constraints may limit the extent*
100 *to which the components may be differentiated from each other. Furthermore, various observational methods of*
101 *the same component could yield differing values. For example, multiple methods for measuring the same*
102 *component could have different intrinsic timescales that are applicable to them, making direct comparisons*
103 *difficult. Improving observational tools for PP, including developing reliable PP error models, is a priority for the*
104 *scientific community, in addition to the modelling issues that are the primary focus of this paper.*

105 Here, we focus mainly on GPP as computed in many ecosystem models. For satellite-based estimates, we
106 treat PP derived from short (1-4 hours) *in situ* incubations as GPP, and those derived from longer (12-24 hour)
107 incubations as NPP, while fully recognising that the distinction is not that clear cut (e.g., Halsey *et al.*, 2011).
108 Furthermore, estimates of the magnitude of losses due to respiration vary considerably. Some estimates place it
109 at about 30% of GPP (e.g., Platt *et al.*, 1991), while some other estimates are higher (e.g., 60% according to Halsey
110 *et al.*, 2011). Platt and Sathyendranath (1988) compared daily water-column PP computed on the basis of short
111 incubations with those measured *in situ* over daily time scales, and showed the two sets of independent estimates
112 to be comparable, which points to low respiration losses. Also, satellite-based estimates of NPP (Behrenfeld and
113 Falkowski, 1997) tend to be roughly the same or higher than GPP estimates (Longhurst *et al.*, 1995). Since, by
114 definition, NPP cannot be greater than GPP, these comparisons reveal a great deal of uncertainty in respiration,
115 or in PP computed using different approaches, when compared with each other.

116

117

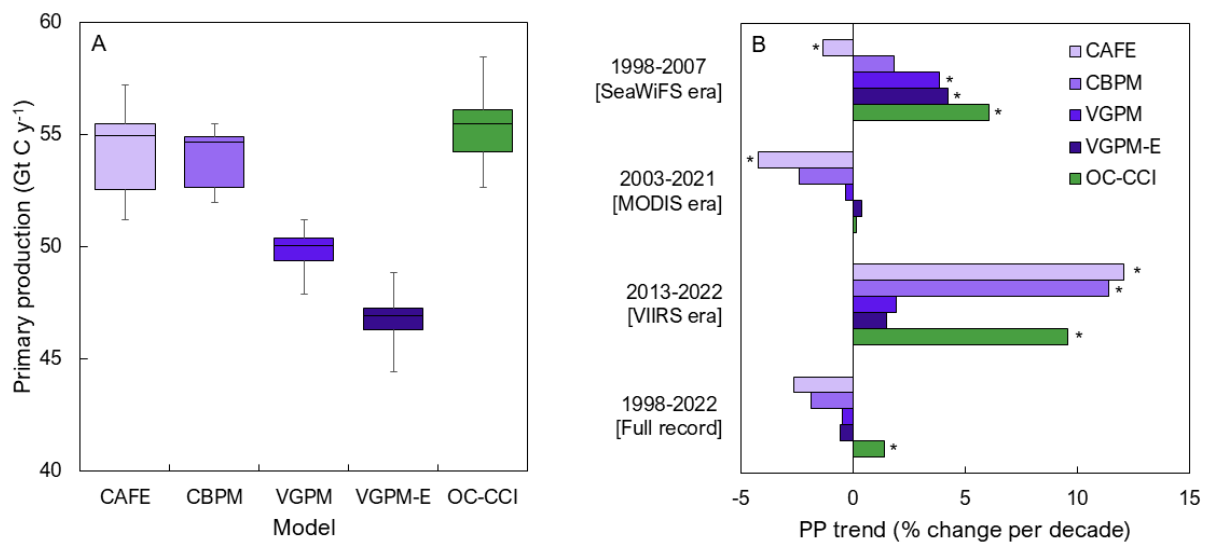
118 **2. Background**

119 Considerable differences exist in model-based estimates (here and elsewhere, we use “models” without a
120 qualifier, to mean both satellite-based and ecosystem models) of the current and past global PP in the ocean, and
121 in ecosystem-model based projections into the future.

122 Satellite-based estimates of global marine PP are converging around 45-55 Pg C y⁻¹ (Figure 1A). These
123 estimates were obtained from both multi-sensor products of the Ocean Colour Climate Change Initiative (OC-
124 CCI; version 6, Sathyendranath *et al.* 2019, Kulk *et al.* 2020, 2021), as well as from single-sensor products of the
125 Oregon State University (<http://orca.science.oregonstate.edu/>), which include the Carbon, Absorption, and
126 Fluorescence Euphotic-resolving (CAFE) model (Silsbe *et al.* 2016; 2025), Carbon-Based Primary Productivity
127 Model (CBPM; Westberry *et al.* 2008), the Vertically Generalised Production Model (VGPM; Behrenfeld and

128 Falkowski 1997) and the VGPM-Eppley model (which incorporates the Eppley (1972) temperature function).
 129 However, we note that much higher values (up to 67 Pg C y⁻¹) and lower values (≤45 Pg C y⁻¹) have also been
 130 reported from satellite-based products (Antoine *et al.* 1996; Behrenfeld *et al.* 2005; Carr *et al.* 2006; Uitz *et al.*
 131 2010) (here we recognise that satellite products may differ in the computed PP components, as noted earlier).

132 Large differences also emerge in the PP trends over the last decades estimated from both the CCI and Oregon
 133 State University products (Figure 1B), as well as associated reanalyses (e.g., those of Gregg and Rousseaux, 2019).
 134 These differences are strongly impacted by the choice of historical period and the underlying characteristics of
 135 the satellite products (e.g., single sensor or multi-sensor), but the choice of satellite-based PP model does matter:
 136 in a recent comparison (Ryan-Keogh *et al.*, 2025) of six satellite-based primary production models applied to a
 137 common satellite product (OC-CCI) and a common period (1998-2023), four of them showed declining trends,
 138 while the other two showed an increasing trend. Interestingly, the split is along the lines of whether the models
 139 incorporated temperature-dependent production parameters, or not. Ryan-Keogh *et al.* (2025) also compared
 140 satellite products with those of several ecosystem models from the Climate Model Intercomparison Project
 141 (CMIP-6), and concluded that, in general, the climate models underestimated the decreasing trends seen in some
 142 of the satellite-based models.
 143

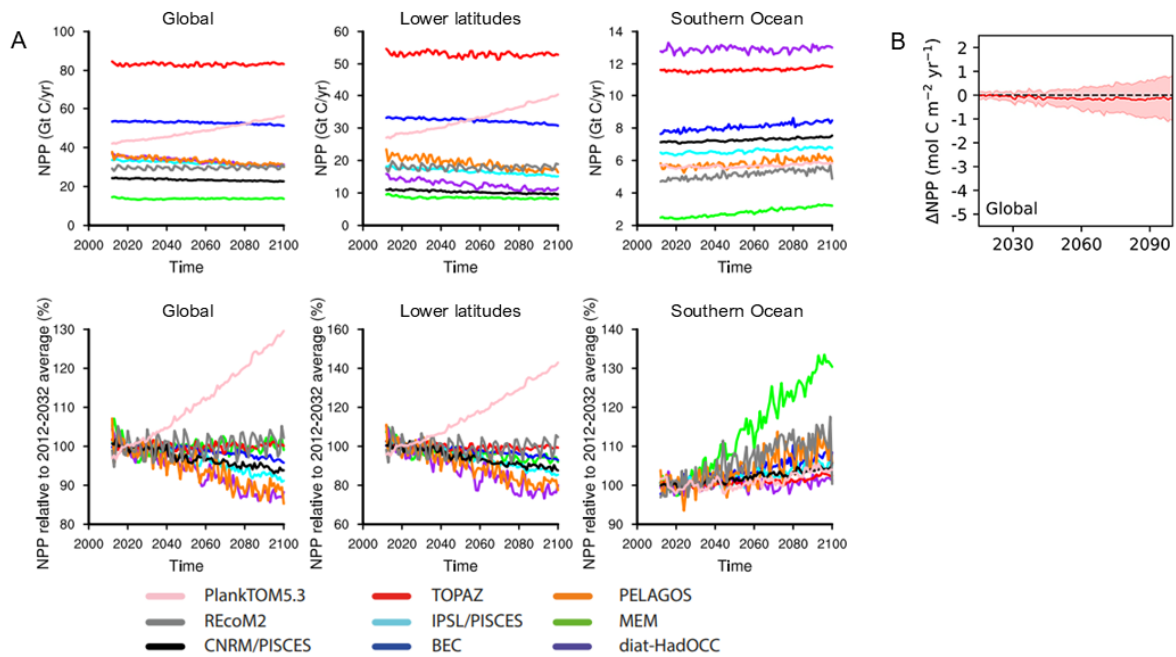


144
 145 **Figure 1.** Global marine PP computed using the satellite-based model of Platt and Sathyendranath (1988) as
 146 updated by Sathyendranath *et al.* (2020) and Kulk *et al.* (2020, 2021) with version 6.0 of Ocean Colour Climate
 147 Change Initiative (OC-CCI) data as input (in green), compared with openly available time-series data from four
 148 other satellite-based primary production models from the Oregon State University Primary Production website
 149 (http://orca.science.oregonstate.edu/-npp_products.php) based on single-sensors: Sea-viewing Wide Field-of-
 150 view Sensor (SeaWiFS; 1998-2007), Moderate Resolution Imaging Spectroradiometer Aqua (MODIS-Aqua;
 151 2003-present), and Visible Infrared Imaging Radiometer Suite (VIIRS; 2013-present). The panels show the
 152 following: A) Global ocean primary production for the five different satellite-based primary production models
 153 for the time period between 1998-2022 (i.e., full data record), for all sensors combined; and B) Trends in primary
 154 production for the full ocean colour data record and for subsets of the periods during which specific sensors were
 155 operational, with stars indicating significant trends ($p < 0.05$), for the five satellite-based primary production
 156 models. All latitudes were considered, but coverage at higher latitudes ($>70^{\circ}\text{N}$ and S) is typically poor in satellite

157 data. Differences in marine PP and its trends are not limited to satellite-based products. Earth System Model
158 intercomparisons show considerably larger uncertainty than the satellite models for the annual NPP estimate
159 during the (recent past) “historical” period (with values reported in the 17-83 Pg C y⁻¹ range; Bopp *et al.*, 2013;
160 Doney *et al.*, 2014; Laufkötter *et al.*, 2015; Tagliabue *et al.*, 2021; see Figure 2), whilst showing weak or no trends
161 over the recent historical period (Kwiatkowski *et al.*, 2020). Ecosystem model uncertainties are even higher in
162 future projections where models disagree even on the sign of change up to the year 2100 under the high emission
163 scenario, although most ecosystem models project a decline in global PP. While the uncertainty in annual NPP in
164 the recent past has decreased in the CMIP6 (Coupled Model Intercomparison Project phase 6) ensemble compared
165 with CMIP5, the uncertainty in projected PP trends has increased significantly in the CMIP6 ensemble compared
166 with CMIP5 (Kwiatkowski *et al.*, 2020). In particular, while the ensemble mean in CMIP5 suggested a significant
167 decrease in PP at the global scale of $-8.06\% \pm 4.83\%$ (where the uncertainties are reported as the inter-model
168 standard deviation), the CMIP6 ensemble has a much smaller mean and the larger standard deviation includes the
169 null hypothesis of no trend ($-1.76\% \pm 9.01\%$). Frölicher *et al.* (2016) have noted that ecosystem model
170 uncertainties (missing/mis-represented processes, parameter uncertainties) dominated the total uncertainty in the
171 21st-century projections of PP and their relative importance with respect to scenario uncertainty does not decrease
172 with projection lead time. Recent studies have confirmed this, highlighting the role of uncertainty in the
173 representation of key biogeochemical processes, including diazotrophy (Tagliabue *et al.*, 2021; Bopp *et al.*, 2022;
174 Doléac *et al.*, 2025), bacterial remineralisation (Kim *et al.*, 2023) and parameter uncertainty (Jones *et al.*, 2024),
175 including in zooplankton grazing rates (Rohr *et al.*, 2023). Laufkötter *et al.* (2015) concluded that the projected
176 future changes in marine PP are driven by multiple processes, including changes in circulation or mixing, leading
177 to a stronger lateral or vertical loss of biomass; increased aggregation or mortality of phytoplankton; or higher
178 grazing pressure. Laufkötter *et al.* (2015) also noted that temperature-dependent functions of PP and loss terms
179 can affect the direction of change of PP from marine ecosystem models in climate warming scenarios. Regional
180 variations in PP are especially sensitive to how models represent this wide range of processes (Dutkiewicz *et al.*,
181 2013), and given the high uncertainty in their model representation, very few of the models agree on the direction
182 of the trend regionally. Furthermore, global models, with their coarse horizontal resolution, struggle to capture
183 coastal and estuarine processes that enhance PP (coastal regions account for 14-33% of global PP; Gattuso *et al.*,
184 1998), which makes them also prone to underestimate global PP.

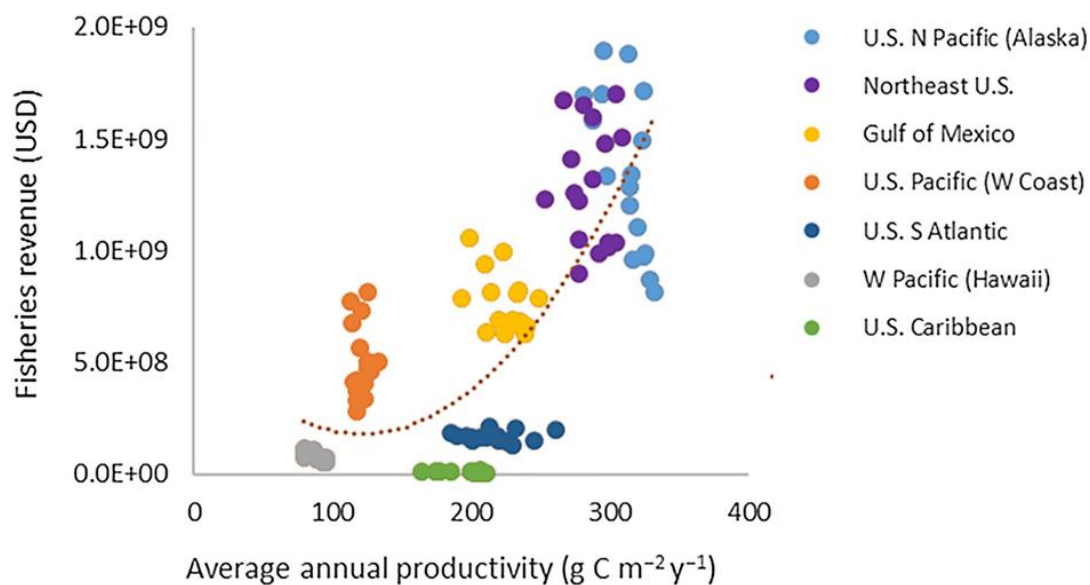
185

186



187
188
189
190
191
192
193
194
195
196
197
198

Figure 2. Comparison of NPP from marine ecosystem models in CMIP5 comparison projected to the end of this century under a high emission scenario. A) From Laufkötter et al. (2015) – RCP8.5 (Representative Concentration Pathways 8.5 scenario), from left to right are global values, lower latitudes (30°S-30°N) and Southern Ocean (90-50°S) in Gt C per year (top) and percent (bottom); and B) Global NPP projections from Tagliabue et al. (2021) – SSP5-8.5 (Shared Socio-economic Pathways 8.5 scenario). Note that the magnitude of contemporary annual NPP ranges from less than 20 to more than 80 Pg C y⁻¹ in the compilation from Laufkötter et al. (2015). Both analyses showed negative and positive global trends, though most ecosystem models predict decreasing trends towards the year 2100.



199
200
201

Figure 3. The impact of PP on fisheries. Figure reproduced from Marshak and Link (2021). Individual observations from different coastal regions of the USA are indicated in different colours.

202 Several studies have also been carried out to compare estimates from ecosystem models with satellite-based
203 products and *in situ* observations, both at global scale (Carr *et al.*, 2006; Steinacher *et al.*, 2010; Bopp *et al.*, 2013;
204 Laufkötter *et al.*, 2015; Séférian *et al.*, 2020; Ryan-Keogh *et al.*, 2025) and at regional scales (Friedrichs *et al.*,
205 2009; Saba *et al.*, 2010; Lee and Yoo, 2016; Doléac *et al.*, 2024). In some cases, these comparisons (e.g., between
206 ecosystem and satellite-based models) led to better constrained PP projections, e.g., in the tropics, using an
207 emergent constraint approach (Kwiatkowski *et al.*, 2017). However, it is fair to say that, overall, these comparisons
208 have not led to convergence of model outputs that would reduce the uncertainty of marine PP estimates. All
209 previous works have highlighted large differences between estimates (e.g., varying from <-60% to >60%; Séférian
210 *et al.*, 2020), with highly variable spatial patterns (Bopp *et al.*, 2013). Tagliabue *et al.* (2021) highlighted the need
211 for stronger constraints on NPP using new approaches that include the growing observational coverage from
212 Biogeochemical-Argo (BGC-Argo) floats (Claustre *et al.*, 2020; for an example of this see Arteaga *et al.*, 2022).
213 Field-based observations of PP, typically treated as the “truth”, are often compared with model outputs to evaluate
214 model performance. However, this type of comparison is confounded by uncertainties in PP measurements, which
215 can be quite high, as well as by the differences in the spatial and temporal scales of the *in situ* observations and
216 the validated models. Furthermore, there are also questions around whether the PP is measured directly, or
217 estimated indirectly. For example, BGC-Argo estimates PP indirectly, inferring it from other, more directly
218 measured variables.

219 Given these challenges both in remote sensing and ecosystem modelling, the IPCC has assigned low
220 confidence to current estimates of marine PP and its trends. The reasons cited include uncertainties in production
221 estimates and projections, the short duration of available time series data used in the analyses, and the lack of
222 independent validation (IPCC 2019; Gulev *et al.*, 2021; Chapter 2 in IPCC AR6, WG I, 2021). This assessment
223 is of particular concern as it has major implications for ecosystem service provision, mitigation planning,
224 enhancing adaptation and building resilience to climate change (Hewitt *et al.*, 2021). These applications often
225 require regional to local information, as PP determines spatial variability in ecosystem services such as fisheries
226 (Marshak and Link, 2021; see Figure 3), but uncertainties increase at these scales compared with global estimates
227 (Tagliabue *et al.*, 2021). Both remote sensing and ecosystem models can, in principle, deliver such regional
228 insights, when used with granularity and resolution needed at the appropriate scales. Reducing uncertainty in
229 models, ideally through a coordinated and internally consistent set of simulations, data and knowledge, would
230 then enable us to discuss downstream services under various climate scenarios and associated risks of tipping
231 points (Jones *et al.*, 2024). Such improvements would support climate policy, as well as management decisions
232 pertaining to climate mitigation and adaptation strategies, at both international and regional levels.

233 We argue here that efforts to reduce uncertainty in estimates and projections of marine PP should include a
234 focus on *investigating model structures and parametrisations*, with the goal of identifying genuine inter-model
235 differences and reconciling apparent differences. In this review, we examine both the sources of differences
236 between satellite-based and ecosystem models, as well as within these two types of models. We argue that there
237 is strong scientific justification for considering how the current model parameterisations could be improved. A
238 straightforward avenue to improvement is that parameters which are currently treated as constants (e.g., the A_i
239 parameters from Table 1) are assigned the most appropriate values consistent with the model structure and with
240 all the available information. A step further is to allow the currently constant parameter values to vary with spatial
241 locations and times. Although variable parameters would increase the complexity of the functional forms used in

242 PP models, we argue that, at least in the less complex PP models (e.g., within satellite models and ecosystem
243 models used in ESMs for climate projections), there are good scientific reasons to expect such parameter variations
244 to be realistic. We propose that absence of such variations is responsible for the many apparent differences
245 between the current PP models. Parameter variability might be less important for the more complex models with
246 large numbers of phytoplankton types and/or size-classes, but for those models it is still essential to focus on the
247 best possible ways of optimising the existing constant parameters. Furthermore, these highly complex models
248 could provide valuable information for estimating the spatio-temporal variability of parameters used in less
249 complex ecosystem and satellite-based models. This would also help increase consistency among different
250 models, making them more comparable. At the same time, caution must be applied to ensure that increased
251 consistency and convergence is not confused with increased accuracy. For this, we would need to continue
252 independent assessments of accuracy, for example by comparisons with *in situ* observations, with full recognition
253 of the caveats that such comparisons entail, as discussed above.

254 In general, we highlight the importance of correct parameterisations that are valid across multiple spatial and
255 temporal scales, and for multiple phytoplankton types. We also discuss the challenges posed by such PP model
256 parametrisations, argue that this is the right time to rise to those challenges, and propose strategies to overcome
257 them. Finally, we discuss uncertainties in marine PP that might persist even when improved model
258 parametrisations are adopted.

259

260 3. Modelling primary production

261 In this section, we assess how marine PP is treated in satellite-based and ecosystem models, identifying inter-
262 model differences.

263 It is useful to consider GPP as the product of a biomass-specific production, say P^M , where M is a measure
264 of phytoplankton biomass, multiplied by the biomass itself. In other words:

$$265 P = P^M \times M, \quad (1)$$

266 such that P^M carries all the information on the physiological controls on PP, whereas M accounts for the role of
267 varying phytoplankton concentrations. Since phytoplankton are complex organisms, many options exist for
268 defining biomass, including concentrations of the phytoplankton pigment chlorophyll-a (B), phytoplankton carbon
269 (C), or nitrogen content. The choice of biomass often depends on practical considerations (such as data
270 availability) or by the study objectives (for example, carbon is an obvious choice in models designed to investigate
271 the biologically mediated carbon cycle in the ocean). Models can also be classified according to which measure
272 of biomass they track as the main currency in the ecosystem.

273 Dimensional analysis suggests that, in its simplest form, P^M can be represented in a canonical form with two
274 parts: a scale factor P_m^M that carries the same dimensions as P^M , and a dimensionless function f_I of the scaled
275 irradiance I_* available for photosynthesis (Platt and Sathyendranath, 1993), where the scaling factor would be a
276 model parameter with the same dimensions as light, such that I_* is dimensionless. Thus, in such a canonical form,
277 P^M can be written as:

$$278 P^M = P_m^M \times f_I(I_*). \quad (2)$$

279 In this form, P_m^M is not strictly constant, but implicitly accounts for the effects of other environmental variables
280 on primary production, such as temperature (T) and nutrients (N), or changes in species composition. Such

281 dependencies can be made more explicit (removing T and N dependence from P_m^M), such that Equation (1)
282 becomes:

$$283 \quad P^M = P_m^M \times F(f_T(T), f_N(N), f_I(I_*)). \quad (3)$$

284 The function $F(f_T, f_N, f_I)$ can be specified as a simple product $f_T \times f_N \times f_I$ (e.g., Laufkötter *et al.*, 2015; Kishi
285 *et al.*, 2006; Vichy *et al.*, 2007; Yool *et al.*, 2013; Butenschön *et al.*, 2016), representing co-limitation by each
286 variable, or it can follow Liebig's law of the minimum (e.g., Gregoire *et al.*, 2008; Daewel and Schrum, 2013;
287 Radtke *et al.*, 2019), where the most limiting resource dictates the growth rate. Note that in Equations 2 and 3, the
288 functions f_i are dimensionless, and that all the dimensions are carried by the scaling factor P_m^M . When models
289 resolve multiple phytoplankton groups or species, Equation 3 is specified for each group, and their contributions
290 are added to get total PP.

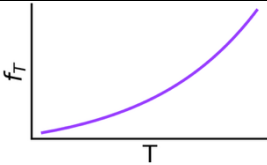
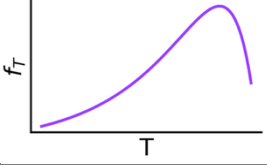
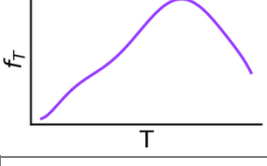
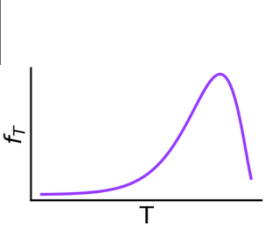
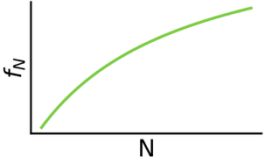
291 Commonly-used functions in PP models that represent the modulating roles of temperature, nutrients and
292 light are summarised in Table 1. When more than one nutrient is considered, additional terms have to be included
293 for each nutrient. Thus, models (the combined functions F) differ depending on (i) how many environmental
294 factors are included in the model, (ii) the explicit functional forms selected for each modulating function; and (iii)
295 the parameter values A_i , D_i assigned to those modulating functions, and whether they are allowed to vary with
296 region and time. Finally, the functions f_i would ideally have values within the $[0,1]$ interval; however, this is often
297 not the case for some of the temperature f_T functions (as can be seen in Table 1).

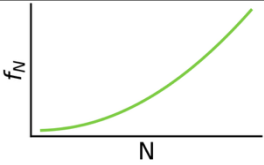
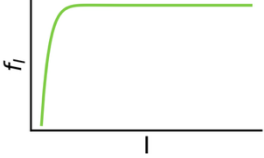
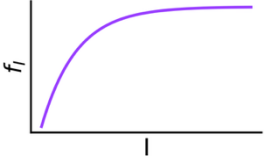
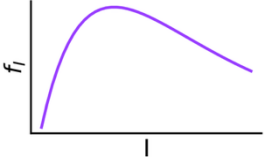
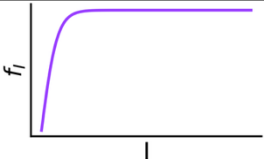
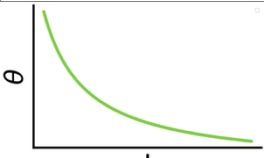
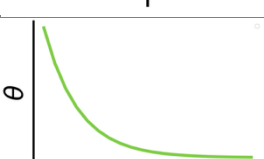
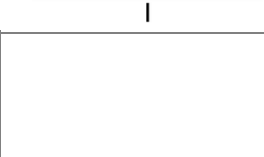
298 In some cases, it is necessary to track multiple measures of phytoplankton biomass within a model. For
299 example, a unit conversion between chlorophyll-a and carbon might be needed to make the exponent in the light
300 function (f_I) dimensionless, or it may be that the model tracks more than one currency. Such a conversion may
301 also be needed to transform modelled phytoplankton carbon fields into chlorophyll-a fields for comparison with
302 satellite-based chlorophyll-a products. This is typically achieved using a chlorophyll-to-carbon ratio (θ), which
303 varies among phytoplankton and under different environmental conditions and is usually estimated using photo-
304 acclimation models. Commonly used functions in photo-acclimation models are also shown in Table 1.

305

306 **Table 1.** The different f_T , f_N , f_I and θ functions used across variety of CMIP and operationally used ecosystem
307 models, as well as satellite models (which however typically do not use an explicit nutrient-limitation function,
308 see Westberry *et al.*, 2008). The ecosystem models explicitly mentioned are Biogeochemical Model for Hypoxic
309 and Benthic Influenced areas (BAHMBI; Gregoire and Soetaert, 2010), Biogeochemical Flux Model (BFM; Vichi
310 *et al.*, 2015), ECOSystem MOdel (ECOSMO; Daewel and Schrum, 2013), European Regional Seas Ecosystem
311 Model (ERSEM; Butenschön *et al.*, 2016), Hadley Centre Ocean Carbon Cycle (HadOCC; Totterdell, 2013),
312 Model of Ecosystem Dynamics, Sequestration and Acidification (MEDUSA; Yool *et al.*, 2013), Marine
313 Ecosystem Model (MEM; Shigemitsu *et al.*, 2012), North-Pacific Ecosystem Model for Understanding Regional
314 Oceanography (NEMURO; Kishi *et al.*, 2007), PELAgic biogeochemistry for Global Ocean Simulations
315 (PELAGOS; Vichi *et al.*, 2007), Pelagic Interactions Scheme for Carbon and Ecosystem Studies (PISCES;
316 Aumont *et al.*, 2015), Carbon, Ocean Biogeochemistry and Lower Trophics (COBALT; Stock *et al.*, 2020, 2025),
317 and DARWIN model (Ward *et al.*, 2012). P_h and N represent the concentrations of phosphate and nitrogen,
318 respectively. Carbon is represented as C , and A_i and D_i stand for the different model parameters. In
319 photoacclimation models, θ is the chlorophyll-to-carbon ratio.

320

Process / Structure	Equation	Description & remarks	Graphical Representation	Examples	Key References
Temperature limitation on photosynthesis	$f_T = e^{A_1 T}$	Exponential temperature dependence on growth rate.		BAHMBI, MEDUSA, NEMURO, BFM, PISCES, PELAGOS, COBALT, DARWIN	Eppley (1972)
	$f_T = Q_{10} \frac{T-A_2}{A_2} - Q_{10} \frac{T-A_3}{A_4}$	Phytoplankton growth rate increases initially exponentially, with enzyme inhibition above optimal temperature		ERSEM	Blackford <i>et al.</i> (2004)
	$f_T = \sum_{i=0}^7 D_i T^i$	Phytoplankton growth rate is represented as an empirical seventh-order polynomial function, fit to observed data.		Vertically Generalised Production Model (VGPM)	Behrenfeld & Falkowski (1997)
	$f_T = A_5 \times e^{A_6 \times T} \times \left(1 - \frac{T-A_7}{A_8}\right)^2$	Function designed to model individual phytoplankton species or types according to their temperature traits, in multi-species models. It has yet to be used routinely in global-scale simulation models, except in a special case of DARWIN.		A version of DARWIN	Norberg (2004), Thomas <i>et al.</i> (2016); Sauterey <i>et al.</i> 2024); Krinos <i>et al.</i> (2025)
	N/A	No explicit temperature dependence is included in the model structure	N/A	ECOSMO, HadOCC	Yumruktepe, Samuelsen, Daewel (2022)
	Empirical assignment	Indirect methods. An example is province-based assignment of parameters	N/A	Satellite P&S, BICEP	Sathyendranath & Platt (1988), Longhurst <i>et al.</i> (1995), Sathyendranath <i>et al.</i> (2020), Kulk <i>et al.</i> (2020)
N-limitation	$f_N = \left(\frac{\left(\frac{P}{C}\right) - A_9}{A_{10} - A_9} \times \left(\frac{\left(\frac{N}{C}\right) - A_{11}}{A_{12} - A_{11}} \right)^{0.5} \right)$	Describes nutrient limitation based on internal nutrient quota for phytoplankton cells. Droop model of cell quota. $0 \leq f_N \leq 1$ depends on the instantaneously calculated internal cell C/N and C/P ratios $\left(\frac{P}{C}, \frac{N}{C}\right)$ and the maximum C/N and C/P ratios (A_5, A_7), having subtracted the structural content of the cell (A_4, A_6) from each.	N/A	ERSEM PISCES (for iron), DARWIN (quota version)	Droop (1974);
	$f_N = \frac{N}{N + A_{13}}$	Michaelis-Menton Equation. Describes N-limitation as a saturating function of external nutrient concentration, and the		NEMURO, ECOSMO, BFM, MEDUSA, HadOCC PISCES (for all nutrients except iron),	Michaelis and Menton (1913), Kovarova-Kovar and Egli (1998), Lee <i>et al.</i> (2015)

		half saturation coefficient A_{13} for that nutrient		DARWIN (monod version)	
	$f_N = \frac{(1-f_A) \times A_{14} \times N}{\left(\frac{(1-f_A) \times A_{14}}{f_A \times A_{15}} + N\right)}$ $f_A = \frac{1}{1 + \sqrt{\frac{A_{14} \times N}{A_{15}}}}$	Optimal uptake kinetics		MEM	Smith <i>et al.</i> (2009)
Light Limitation	$f_I = I \times e^{1-A_{16} \times I}$	Photosynthesis rate increases then declines at high light intensities due to photoinhibition.		NEMURO	Steele (1962)
	$f_I = (1 - e^{-A_{17} \times I})$	Photosynthesis follows a light saturation curve with no inhibition at high light levels		Satellite	Platt <i>et al.</i> (1980; 1990) Sathyendranath <i>et al.</i> (2020); Kulk <i>et al.</i> (2020)
	$f_I = (1 - e^{-A_{18} \times I}) \times e^{-A_{19} \times I}$	Photosynthesis follows a light saturation curve with inhibition at high light levels.		BAHBI, MEM	Platt <i>et al.</i> (1980)
	$f_I = \tanh(A_{20} \times I)$	Model with no photoinhibition. A hyperbolic tangent function is used to simulate light saturation curve.		ECOSMO	Jassby & Platt (1976)
Photo-acclimation	$\theta = \frac{A_{21}}{\left(1 + \frac{A_{21} A_{22} I}{2A_{23}}\right)}$	Photo acclimation model based on the concept of resource allocation, with maximum Chl-to-carbon ratio reached as light approaches zero.		ERSEM, BFM, PISCES, PELAGOS, COBALT, DARWIN	Geider <i>et al.</i> (1997,1998)
	$\theta = 0.022 + (0.045 - 0.022)e^{-3I} - g(N, T)$	The Chl-to-carbon ratio (θ is determined by photoacclimation, and also by nutrient and temperature stress.		CBPM	Westberry <i>et al.</i> (2008)
	$\theta = \frac{A_{25}}{I \times A_{24}^{-1}} \times \left(1 - e^{-(I \times A_{24}^{-1})}\right)$	Based on an extended version of Geider <i>et al.</i> (1997,1998) photoacclimation model. Uses the exact analytic solution to the Guider <i>et al.</i> (1997) model Jackson <i>et al.</i> (2017), extended to to account for spectral light effects (Sathyendranath <i>et al.</i> 2020). It incorporates photo-acclimation effects on the chlorophyll-to-carbon ratio		Satellite	Sathyendranath <i>et al.</i> (2020), Jackson <i>et al.</i> (2019), Zheng <i>et al.</i> (2025)

322 In the next two sections, we examine in more detail the variety of ways in which these concepts are implemented
323 in satellite-based and ecosystem models.

324

325 3.1 Satellite-based models

326 In satellite-based PP models, daily water-column production is calculated as a function of phytoplankton biomass
327 and light available at the sea surface, obtained from ocean-colour remote-sensing observations, coupled with
328 models of photosynthetic response to light. Since the launch of the first ocean-colour satellite, the Coastal Zone
329 Color Scanner (CZCS) in the 1970s, scientists have developed various satellite-based PP models that can be
330 roughly categorised into three classes: 1) Chlorophyll-based models, 2) Absorption-based models, and 3) Carbon-
331 based models (Figure 4). Each of these models could be further classified according to whether they are
332 implemented as linear/non-linear, spectral/non-spectral, vertically-uniform/vertically-non-uniform, or as a
333 combination of these (Platt and Sathyendranath, 1993; Sathyendranath and Platt, 2007). Further bifurcations
334 occur, depending on whether the models are depth-integrated, or not (Friedrichs *et al.*, 2009). Most of the satellite-
335 based models do not resolve PP by phytoplankton size classes, or functional types, with some exceptions, such as
336 Uitz *et al.* (2010), Brewin *et al.* (2016) and Tao *et al.* (2017).

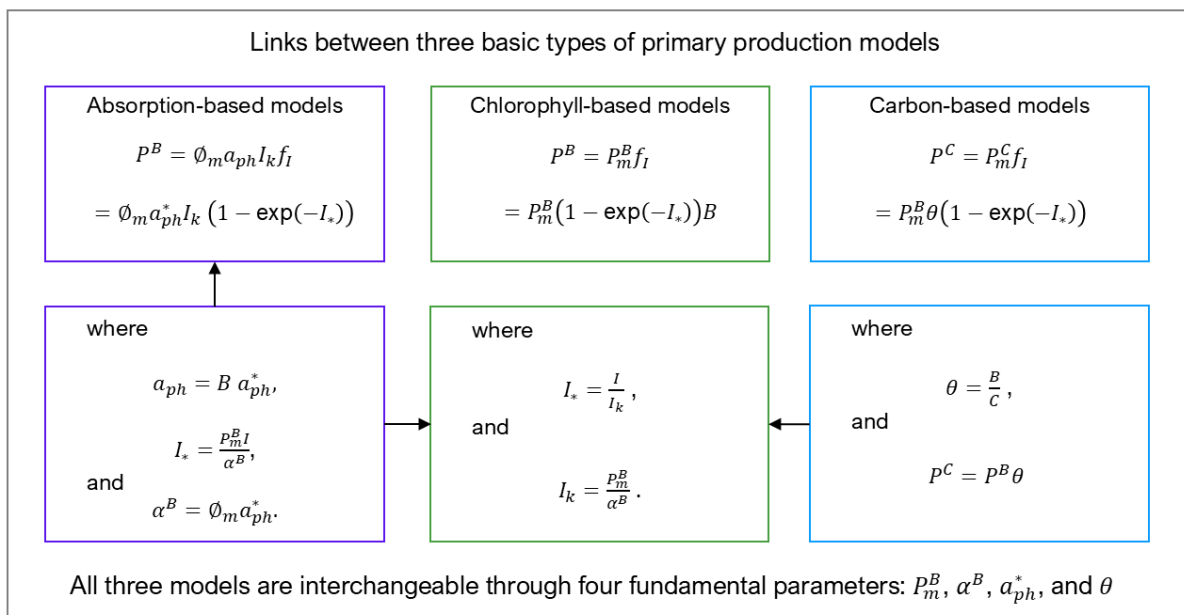
337 Satellite-based model outputs have been compared against *in situ* data, both globally and regionally
338 (Friedrichs *et al.*, 2009; Saba *et al.*, 2010, Lee *et al.*, 2015). No clear new directions have emerged from these
339 intercomparisons. [A contributing factor to this outcome could be the uncertainty in field measurements of PP and](#)
340 [also to issues related to mismatches between the temporal and spatial resolutions of models and observations.](#)
341 These inter-comparisons did not examine closely the role of model parameters in the divergence of outputs.
342 However, the assignment of model parameters remains one of the biggest sources of uncertainty in estimates of
343 primary production from remote sensing observations (Platt and Sathyendranath, 1993; Sathyendranath and Platt,
344 2007; Sathyendranath *et al.*, 2009; Kulk *et al.*, 2020, 2021; Brewin *et al.*, 2023).

345 Interestingly, the types of models described above all converge to the same principles and a common set of
346 parameters (Sathyendranath & Platt, 2007; Figure 4). Chlorophyll-based (or available-light or photosynthesis-
347 irradiance) models typically use the parameters of the photosynthesis-irradiance curve, normalised to B, the
348 concentration of chlorophyll-a, i.e., the initial slope (α^B) and the assimilation number (P_m^B) of the light saturation
349 curve, and the photoacclimation parameter ($I_k = P_m^B/\alpha^B$) derived from the other two (Platt *et al.*, 1980;
350 Sathyendranath and Platt, 2007; Figure 4). Absorption-based (which are also called biomass-independent or
351 inherent-optical-property) models use the realised maximum quantum yield (ϕ_m) and the absorption coefficient
352 of phytoplankton (a_{ph}) (Kiefer & Mitchell, 1983, Lee *et al.*, 2015). This model can be shown to be equivalent to
353 the photosynthesis-irradiance models by using the identity $\phi_m = \alpha^B/a_{ph}$ (Platt *et al.*, 1988; Sathyendranath and
354 Platt, 2007; Figure 4). The key parameter in carbon-based (or growth) models is the growth rate (g), i.e., the rate
355 of change of carbon per unit time normalised to the initial phytoplankton carbon concentration. The chlorophyll-
356 to-carbon ratio (θ) can be used to transform growth models to production models and vice versa (Sathyendranath
357 and Platt, 2007; Sathyendranath *et al.*, 2009). Thus, the different types of satellite-based primary production
358 models are interchangeable through a common set of parameters: the initial slope (α^B) and assimilation number
359 (P_m^B) of the light saturation curve, the mean specific absorption coefficient of phytoplankton (a_{ph}^*), and the
360 chlorophyll-to-carbon ratio (θ) (Sathyendranath and Platt, 2007; Sathyendranath *et al.*, 2009). When the light
361 incident at the sea surface exceeds a threshold above which light can damage the photosystems, a photo-inhibition

362 term has to be added to the photosynthesis-irradiance equation (Platt *et al.*, 1980). This parameter is often not used
 363 in satellite-based models; a sensitivity analysis on a photosynthesis-irradiance model (Platt *et al.*, 1990) showed
 364 that incorporation of realistic values of the photo-inhibition parameter into the model had only small to negligible
 365 effect on computed water-column primary production, which lends some justification to why this term is often
 366 ignored. But this is a simplification that can be readily dropped, if new evidence suggests that photo-inhibition
 367 could be important at large scales.

368 Spectral models of primary production are designed to capture the wavelength-dependent light penetration
 369 underwater, and wavelength-dependent photosynthesis (Sathyendranath and Platt, 1989). In fully-spectral models,
 370 the action spectrum of photosynthesis (which describes the wavelength-resolved values of the initial slope α^B) is
 371 coupled to the light available at corresponding wavelengths for photosynthesis (Sathyendranath and Platt, 1989;
 372 Kyewalyanga *et al.*, 1992), such that the product $\alpha^B I$ that appears in non-spectral models has to be replaced by
 373 the wavelength integral $\int \alpha^B(\lambda) I(\lambda) d\lambda$, where λ represents the wavelength, and the integral is taken over the
 374 photosynthetically active range (400-700 nm). The spectral form of the action spectrum closely resembles that of
 375 the phytoplankton absorption spectrum (a_{ph}) (Sathyendranath *et al.*, 1989b; Kyewalyanga *et al.*, 1997). Spectral
 376 effects are generally considered to be not relevant at saturating light levels. Under light-limiting conditions, if the
 377 light available is blue-rich, where the action spectrum has a maximum, the coupling between light and
 378 photosynthesis would be stronger than if the light were green-rich, where the action spectrum typically goes
 379 through a minimum. We know from previous studies that spectral and non-spectral models may differ from each
 380 other in a systematic manner (Sathyendranath and Platt, 2007), because non-spectral models are not able to
 381 account for the covariance (or the lack of it) between spectrally-resolved α^B and a_{ph} . To some extent, the impact
 382 of the spectral effects on water-column primary production could be accommodated into non-spectral models by
 383 suitably tuning the parameters of non-spectral models (Platt and Sathyendranath, 1991). Typically, therefore, one
 384 anticipates systematic differences between spectral and non-spectral models of marine primary production, unless
 385 model parameters are adjusted to compensate for the difference.

386



387

388 **Figure 4.** Phytoplankton absorption-, chlorophyll-a- and carbon-based primary-production models commonly-
 389 used in satellite-based approaches, and the parameter transformations between them. Notations: Primary
 390 production (P), light-limitation function (f_l), as in Table 1, assimilation number of the saturation-light curve, or
 391 the light saturation parameter (P_m^B), initial slope of the light-saturation curve (α^B), mean absorption coefficient of
 392 phytoplankton (a_{ph}), chlorophyll-to-carbon ratio (θ), chlorophyll-specific absorption coefficient of
 393 phytoplankton (a_{ph}^*), realised maximum quantum yield of photosynthesis (Φ_m), photoacclimation parameter of
 394 the light-saturation curve (I_k), phytoplankton biomass in chlorophyll-a units (B), normalised irradiance (I_*),
 395 irradiance (I), phytoplankton carbon biomass (C), time (t), and growth rate (g). One of the (f_l) functions from
 396 Table 1 was selected here for illustrative purposes, but other functions have also been used in the literature. As
 397 shown below (Figure 7), numerically, most of the (f_l) functions are almost identical to each other, unless photo-
 398 inhibition is introduced. Currently, remote-sensing-based primary-production models do not incorporate the
 399 photo-inhibition term.

400

401 3.2 Ecosystem models

402 Ecosystem models differ greatly in their complexity, ranging from simple, three-component Nutrient-
 403 Phytoplankton-Zooplankton (NPZ) models (Fasham *et al.*, 1990; Steele and Henderson, 1992; Franks, 2002;
 404 Gentleman, 2002) to highly complex ones with hundreds of ecosystem components (e.g., Dutkiewicz *et al.*, 2020,
 405 Fennel *et al.*, 2022). Some models use a single measure for biomass (e.g., carbon), and a single nutrient (usually
 406 nitrogen) as the model currency, assuming a fixed stoichiometry (relationship between biogeochemically-
 407 important elements), whereas other models allow for dynamically resolved stoichiometry within f_N . In this
 408 section, we focus primarily (but not exclusively) on marine ecosystem models (here used interchangeably with
 409 “marine biogeochemical models”) that participate in the Climate Model Intercomparison Project (CMIP) (e.g.,
 410 Laufkotter *et al.*, 2015; Kwiatkowski *et al.*, 2020), as well as regional ecosystem models that are run operationally
 411 by forecasting centres (e.g., Fennel *et al.*, 2019) for regional climate projections. In these models, PP is usually
 412 estimated along the lines of Equations 2 and 3, where primary production (P) is calculated by multiplying the
 413 phytoplankton biomass (usually carbon) by its reference growth rate g , modulated typically by the three
 414 functions, f_T , f_N and f_l .

415 There are also many similarities across the ecosystem models that go beyond the functional form of Equation
 416 2, and a few common approaches can be identified in the equations used to express the functions f_T , f_N and f_l
 417 (Table 1). For instance, f_T is typically described through an exponential function (originating from Eppley, 1972;
 418 e.g., see Laufkotter *et al.*, 2015), that was proposed as an outer envelope of temperature response functions of
 419 many single phytoplankton species (Eppley, 1972; Norberg, 2004). The response functions of individual
 420 phytoplankton species could include inhibition temperatures higher than what is optimal for growth of that specific
 421 species (e.g., Norberg, 2004; Butenschön *et al.*, 2016, Dutkiewicz *et al.*, 2020a), which is linked to Q10, a measure
 422 of the sensitivity of photosynthesis to temperature. This temperature inhibition of individual phytoplankton
 423 species is not captured by the exponential function representing the collective response. Furthermore, ecosystem
 424 models that resolve groups of phytoplankton (e.g., diatoms) do not have temperature inhibition, with the implicit
 425 assumption that there is a spectrum of diatoms that have temperature optima across the full temperature range (see
 426 e.g., Anderson *et al.*, 2020). Furthermore, some models do not have explicit PP temperature dependence at all
 427 (e.g., Daewel and Schrum, 2013). When multiple nutrients are considered, the f_N function is typically formulated

428 to use Liebig's law of minimum to combine their effects on PP, and is often based either on cell quota of nutrients
429 within the cells (Droop, 1974), or on the concentrations of the nutrients in the medium (Michaelis and Menten,
430 1913). In some cases (e.g., Shigemitsu *et al.*, 2012), f_N is based on the optimal nutrient uptake kinetics (Smith *et*
431 *al.*, 2009), which allows for parameters in the Michaelis-Menten equation to vary (Table 1). A variety of equations
432 are currently in use to describe the light-dependence function (f_I , see Table 1) in ecosystem models, including
433 those from Platt *et al.* (1980), Steele (1962), and Jassby and Platt (1976), some of which account for the effect of
434 photo-inhibition at high light, whilst others do not. Furthermore, many of the ecosystem models also include
435 photoacclimation, either as part of the f_I function, or as an additional term, mostly following the model of Geider
436 *et al.* (1997, 1998).

437 Other significant differences across ecosystem photosynthesis models include the number of phytoplankton
438 functional types and size-classes represented, the number of limiting nutrients included (and the types of equations
439 selected to represent the role of each nutrient), and the number of wavebands considered in representation of
440 irradiance (the level to which light is spectrally and directionally resolved, e.g., see Platt and Sathyendranath,
441 1991; Dutkiewicz *et al.*, 2015; Gregg & Rousseaux, 2016). Practically all ecosystem models include nitrogen
442 limitation. But iron limitation is also considered important, as is silica limitation, especially in those models that
443 include diatoms as a phytoplankton class. Phosphate limitation becomes important as well, in particular when
444 dealing with nitrogen-fixing organisms. Another fundamental difference lies in the representation of the
445 production and remineralisation of particulate and dissolved organic matter which are included in the models as
446 explicit or implicit processes, affecting the model parametrisations of GPP, which may or may not include
447 exudation (e.g., Butenschön *et al.*, 2016; Vichi *et al.*, 2007; Wu *et al.*, 2021).

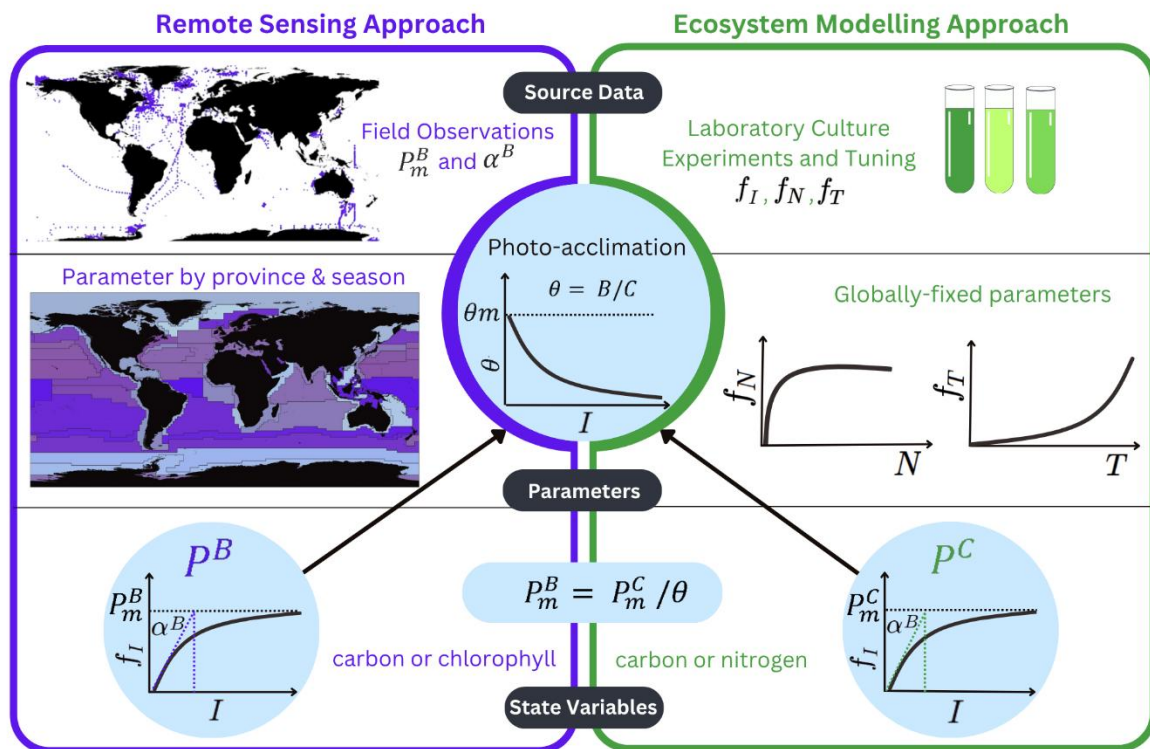
448

449 **3.3 Comparison of satellite-based and ecosystem models**

450 Satellite-based and ecosystem models for estimating ocean PP have some similarities, but also key distinctions
451 (Figure 5; also see IOCCG, 2020). Model parameter assignment provides one clear perspective on a difference
452 between the two types of models. For example, parameters associated with PP models in the satellite-based
453 approach of Platt and Sathyendranath (1988), Kulk *et al.* (2020) and Sathyendranath *et al.* (2020) are established
454 from field observations, whereas ecosystem model parameters are typically estimated using information from
455 laboratory experiments conducted under controlled conditions, followed by tuning the model towards the available
456 observations. But here also, the distinction is not clear cut: for example, the carbon-based production model of
457 Behrenfeld *et al.* (2005) relies on culture measurements to establish growth rate and carbon-to-chlorophyll ratio.
458 Some satellite-based models that do not have explicit nutrient and temperature dependencies implicitly
459 incorporate those dependencies in the model parameter values, which are allowed to vary across biogeographical
460 provinces (Longhurst, 2007) and seasons (e.g., see Figure 6 for photosynthesis-irradiance parameter data
461 partitioned according to Longhurst provinces), representing different nutrient and temperature environments.
462 Ecosystem models typically represent the nutrient and temperature limitation explicitly, with different parameters
463 assigned to each plankton group. Another difference in parameterisation is that many ecosystem models use
464 maximum carbon or nitrogen-specific production rate under optimal conditions as a model parameter and the
465 corresponding biomass is then used to scale PP to its absolute value (Figure 5). While carbon-based satellite
466 algorithms for PP are similar to ecosystem models in this respect, other satellite models rely on bio-optical
467 properties such as chlorophyll-a concentration or phytoplankton absorption coefficient as the state variable. Some

468 ecosystem models also include a photo-inhibition term, to represent the reduction in photosynthesis under high
 469 light intensities, whereas satellite-based models typically account only for the saturating response to light without
 470 including photoinhibition. Photoacclimation is generally addressed by both approaches, with many of them
 471 relying on variations of the Geider *et al.* (1997, 1998), though there are exceptions (e.g., photoacclimation model
 472 in Westberry *et al.*, 2008).

473 Finally, the ecosystem models are able to compute depth-resolved PP, as is the case for the satellite-based
 474 method proposed by Platt and Sathyendranath (1988), whereas some other satellite-based models are designed to
 475 yield vertically integrated production (e.g., Behrenfeld and Falkowski, 1997).



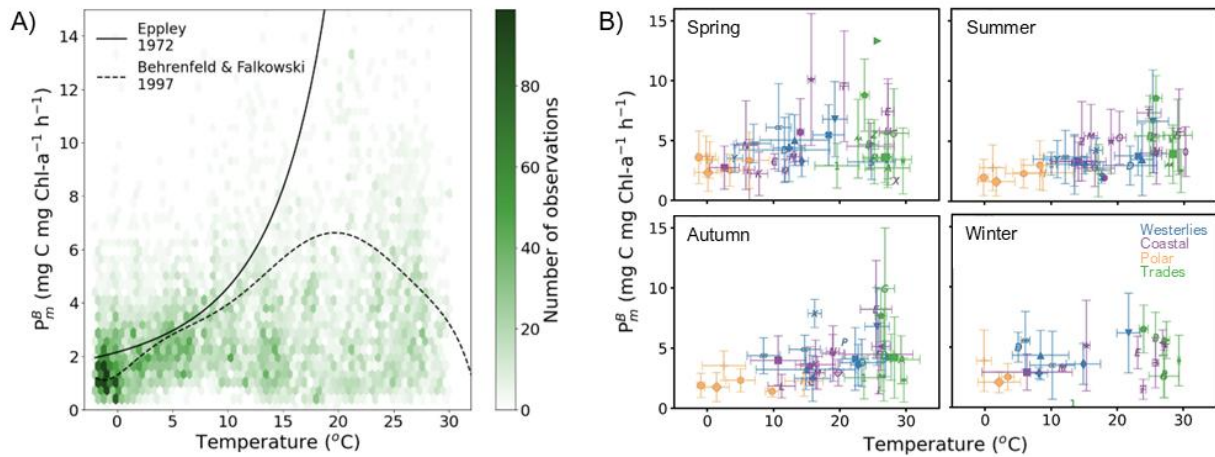
476
 477 **Figure 5.** Comparison of satellite remote sensing (left) and ecosystem modelling (right) approaches to computing
 478 marine primary production, and where they interact (light blue) through the photo-acclimation model which is
 479 essential to enable comparison between the models. I = Light, N = Nutrient, T = Temperature. It should be noted
 480 that although carbon, or nitrogen, are the most common currency used by the ecosystem models, there are also
 481 ecosystem models which use chlorophyll-a as the currency.

482
 483 All satellite-based models are data-rich, in the sense that they are designed to exploit satellite observations,
 484 typically with global coverage and nominal daily repeat frequency. Some use culture data as auxiliary information;
 485 others rely on *in situ* field observations. Ecosystem models, on the other hand, tend to be data-sparse; even when
 486 operated in data assimilation mode, only a fraction of the modelled ecosystem compartments or fluxes are usually
 487 constrained by assimilation. The constraints imposed by satellite data availability limit the processes and variables
 488 that can be estimated, whereas ecosystem models tend to be rich in outputs they provide.

489 Platt and Sathyendranath (1997) proposed a hierarchy of PP models (Figure 7). Almost all the types of models
 490 in this hierarchical classification, other than purely statistical models, are represented in PP models under
 491 discussion in this paper. With the exception of absorbed-light models that are in use in satellite-based models, but
 492 not in ecosystem models, the different classes of models are found in both types of models. In this regard, the
 493 diversity of models within satellite-based or ecosystem-based approaches is no smaller than across those two
 494 groups of models, though, notably, models that use chlorophyll-a as the state variable are unique to satellite-based
 495 approaches. (There are sound reasons for the choice of chlorophyll-a concentration as the state variable, in addition
 496 to the obvious one that it is readily available from ocean-colour data, e.g., Sathyendranath *et al.*, 2023.)

497 When dealing with complex problems such as the one addressed here, it is always an advantage to look at the
 498 problem from multiple angles. Convergence of solutions add confidence, divergence helps identify sources of
 499 discrepancy. It is worth emphasising that the relative strengths and weaknesses of ecosystem and satellite-based
 500 models can be leveraged, once the two types of models become better integrated, as advocated in this paper. We
 501 provide concrete examples on how the two types of models could be of benefit to each other in the section outlining
 502 the way forward.

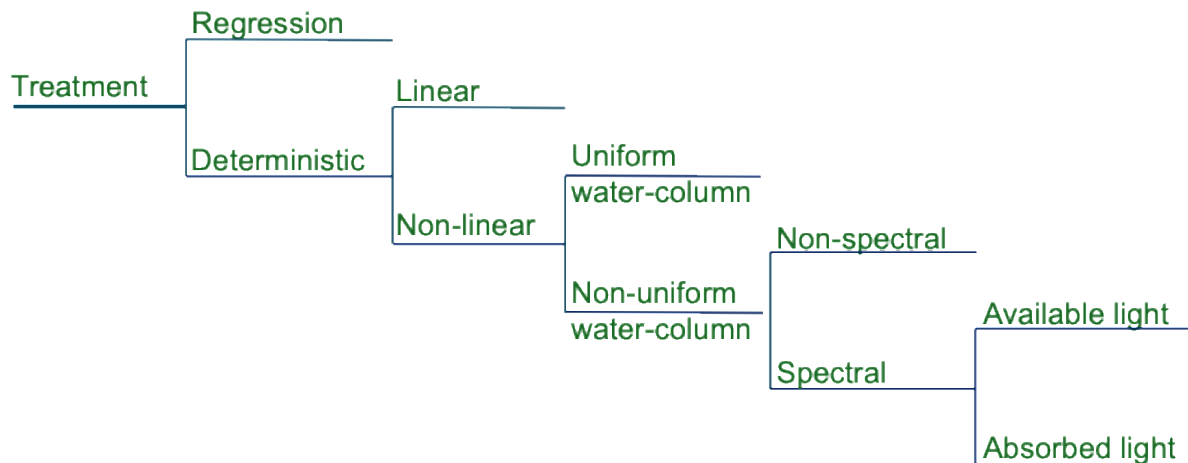
503



504

505 **Figure 6.** Variability in the photosynthesis-irradiance parameter P_m^B in the ocean. A) Parameter values from a
 506 global in situ dataset (Bouman *et al.* 2018; Kulk *et al.* 2020) plotted as a function of temperature. Two commonly-
 507 used temperature-dependent equations (Eppley 1972; Behrenfeld and Falkowski 1997) of this parameter are also
 508 shown. B) The same data sorted according to ecological provinces of Longhurst (2007) and according to season,
 509 with colours representing four different oceanic biomes (Longhurst 2007), showing that some structure and pattern
 510 emerge when the data are organised according to oceanic biomes and to a smaller degree seasons.

Hierarchy of Primary Production Models



511

512 **Figure 7.** Hierarchy of primary production models. The models get more complete (and more complex), as we go
 513 from left to right, and from the upper to the lower limb of each branch.

514

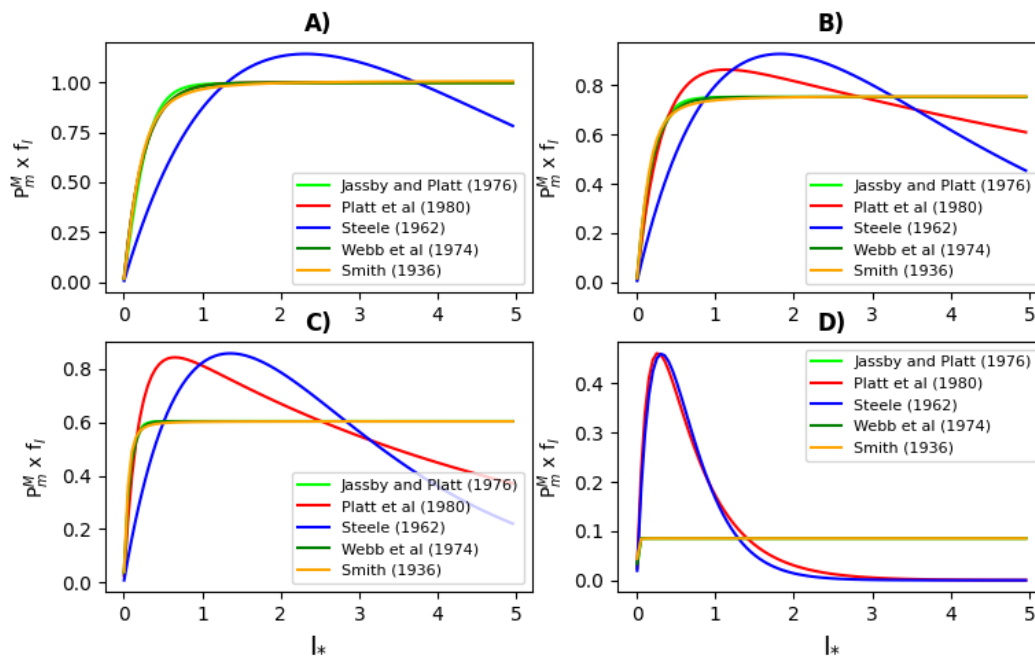
515

516 4. How similar are the different primary production models?

517 Platt and Sathyendranath (1993) showed that we can anticipate systematic biases between satellite-based models
 518 that are structured differently, and we can theoretically, or numerically predict under what conditions the biases
 519 relative to each other will manifest themselves. For example, linear and non-linear models are expected to behave
 520 similarly under low-light levels, but to diverge as light levels increase. The authors also showed that when PP
 521 models have similar structures, it is possible to reduce all of them to a common, canonical form, revealing that
 522 apparently-different model types (available light models, absorbed light models, chlorophyll-based or carbon-
 523 based models) become equivalent when implemented with comparable model parameter values (Platt and
 524 Sathyendranath, 1993; also see Sathyendranath and Platt, 2007; Sathyendranath *et al.*, 2020). Such comparisons
 525 also reveal systematic biases between spectral and non-spectral models of PP, arising from spectral effects in both
 526 underwater light penetration and phytoplankton light utilisation. It has been demonstrated that biases between
 527 spectral and non-spectral PP models can be minimised by tuning the diffuse attenuation coefficient of
 528 downwelling irradiance, which determines the rate of change of available light with depth (Platt and
 529 Sathyendranath, 1991; Kyewalyanga *et al.*, 1992). Similarly, Kovač *et al.* (2016a) demonstrated that a locally
 530 tuned non-spectral model, with adjusted values of photosynthesis parameters, can outperform a spectral model,
 531 without locally tuned values of photosynthesis parameters. Such comparisons bring to the fore the importance of
 532 parameter assessment, assignment, and evaluation to understand model performances, uncertainties and
 533 divergences, which is at the core of this review.

534 To illustrate the point, let us focus, for example, on the light function (f_i), which takes a wide range of forms
 535 in the literature (see Table 1). Even though the functional forms cannot be analytically transformed into each other
 536 (they are mathematically different), numerically they could still be very close to each other, in the sense that they
 537 can all fit the same observations similarly well when the parameters are chosen appropriately (Kovač *et al.*, 2017).
 538 These different forms split into two classes: one that includes photo-inhibition and the other that does not (Amirian
 539 *et al.*, 2025). Figure 8 shows that the f_i models without photo-inhibition (Webb *et al.*, 1974; Jassby and Platt,

540 1976; Smith, 1936) are all practically identical to each other for equivalent parameter values and are therefore
 541 basically indistinguishable from each other. It should also be noted that the Webb *et al.* (1974) model is a special
 542 case of the Platt *et al.* (1980) model for the case of zero photo-inhibition. The f_i model that stands out is the one
 543 of Steele (1962), which struggles to match the other f_i models under low-light conditions. However, when photo-
 544 inhibition is important, the f_i model of Platt *et al.* (1980) can again nicely match the Steele (1962) model if their
 545 parameter values are chosen appropriately. What we learn from Figure 8 is that a lot of the diversity in f_i models
 546 is only apparent, as the diversity can be eliminated via model parametrisation.



547
 548 **Figure 8.** Comparing the functional forms of four f_i models in different regimes. Since only the functional forms
 549 are compared, the x and y axes do not necessarily represent realistic values of normalized irradiance (I_*) or f_i , and
 550 the units are arbitrary. The Figure shows the degree to which the five different models can be "tuned" to each
 551 other through fitting their parameters in a suitable way. The functional forms for the f_i models presented in this
 552 figure are introduced in Tab.1, except the model by Webb *et al.* (1974), which is a special case of Platt *et al.*
 553 (1980) for zero photoinhibition (setting $A_{14} = 0$, see Tab.1). Furthermore, what is plotted in this figure is f_i
 554 multiplied by the scaling factor P_m^M in Equations 2 and 3. The panels A-D show cases of increasing photoinhibition
 555 as modelled by the most complex Platt *et al.* (1980) model (A is the lowest, D the highest), with the other models
 556 tuned to best fit the curve corresponding to Platt *et al.* (1980). We see that the five models essentially split into
 557 two families, each representing well a limiting case of either no photoinhibition (Jassby and Platt 1976, Webb *et al.*
 558 *al.* 1974, Smith 1936), or very high photoinhibition (Steele 1962).

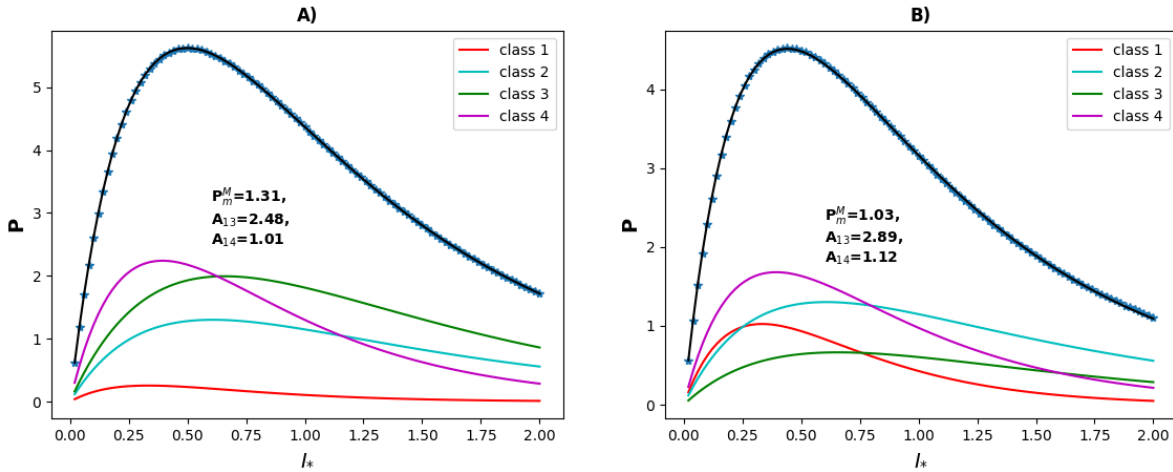
559

560 In general, PP models are designed to represent limitations to phytoplankton growth (whether from light,
 561 nutrients or temperature) under different environmental conditions and for different groups of phytoplankton, as
 562 appropriate. These models have the potential to be generalised to deal with additional external conditions (which
 563 may not be explicitly included in the model) by incorporating spatially and temporally variable parameter values.
 564 This flexibility allows models to account for the diversity of phytoplankton and the processes responsible for their
 565 dynamics, which are not explicitly represented in current models. Representing the full diversity of phytoplankton

566 species is not feasible due to lack of understanding and computational demand, which is why models typically
567 rely on the use of phytoplankton classes to represent aggregations of multiple species based on shared
568 characteristics or traits, such as body size, biogeochemical functions, life strategies and behaviours. This approach
569 captures at best the average or most typical behaviour of each class (e.g., Anderson, 2020; Ratnarajah *et al.*, 2023).
570 When aggregating species according to their physiological and functional traits and behavioural patterns into a
571 pre-defined number of modelled classes, fixed values are assigned to model parameters within each aggregated
572 class. For ecosystem models, many of these parameters have assigned values based on laboratory or mesocosm
573 experiments (Geider *et al.*, 1998; Schartau *et al.*, 2017; Ratnarajah *et al.*, 2023), often focusing on a small number
574 of carefully-selected species, far from capturing the full diversity of organisms or their responses and behaviours
575 that might be expected in the natural environment across large spatio-temporal scales (Geider *et al.*, 1998;
576 Schartau *et al.*, 2017; Ratnarajah *et al.*, 2023). In contrast, in the natural environment, we can expect parameters
577 to vary in time and space, reflecting both changes in the governing conditions and in the unresolved functional
578 diversity in the makeup of modelled planktonic communities (Schartau *et al.*, 2017). Such parameter variability
579 can be observed in model calibration experiments (e.g., Leeds *et al.*, 2011; Mattern *et al.*, 2012, 2014), including
580 those using data assimilation to estimate model parameters jointly with the model state (e.g., Pastres *et al.*, 2003;
581 Tijputra *et al.*, 2007; Roy *et al.*, 2012; Doron *et al.*, 2013; Simon *et al.*, 2015; Gharamti *et al.*, 2017a,b; Skákala
582 *et al.*, 2024).

583 A simple illustration of how parameter variability emerges from aggregating species into classes is provided
584 in Figure 9. Although models differ from each other in the number of phytoplankton classes they resolve, for each
585 phytoplankton class they typically use the same functional form to describe photosynthesis, with total
586 phytoplankton PP corresponding to the sum of contributions across all classes. Figure 9 demonstrates that models
587 with different numbers of classes become equivalent in their description of total PP, provided that the parameters
588 in models with fewer classes are allowed to vary with space and time. In such a way, spatio-temporal parameter
589 variations could effectively capture the influence of unresolved diversity in phytoplankton community structure,
590 in models with only a few phytoplankton classes. The spatio-temporal model parameter variations would then be
591 a consequence of the models' inability to sufficiently resolve phytoplankton species, which also means that such
592 parameter variability would be expected to be especially relevant for the simpler models (e.g., ecosystem models
593 typically used in ESMs). The more complex models currently in use (e.g., DARWIN; see Ward *et al.*, 2012;
594 Dutkiewicz *et al.*, 2020a) would have less reason to adopt spatio-temporally variable parameters; but these models
595 are typically too computationally expensive to be run as part of ESMs in long-term ensemble-based climate
596 projections. Furthermore, even as complex as they are, they still represent only a fraction of the real-world
597 diversity. On the other hand, as the models get more complex by incorporating more ecosystem compartments,
598 the challenge shifts to calibrating each of the large numbers of parameters to adequately capture the functions of
599 each of the model components.

600



601

602 **Figure 9.** A simple illustration of how unresolved phytoplankton community structure can lead to parameter
 603 variability. In both panels, we plot PP expressed as $P = P_m^M \cdot f_I(I_*)$. M with functional form f_I corresponding to
 604 the Platt *et al.* (1980) model (see Tab.1). As in Fig. 8, ranges of scaled irradiance, I_* , and PP values are arbitrary.
 605 Four phytoplankton classes are plotted, each with different P_m^M, A_{13}, A_{14} parameters. The dark blue dots are
 606 obtained by summing up the PP across the four classes (this corresponds to PP of total phytoplankton) and the
 607 dark blue line is the fit of the points with the same functional form used for the four phytoplankton classes
 608 assuming the total phytoplankton concentration is the sum of the concentrations of the four classes. The two panels
 609 show two situations where the same total phytoplankton concentration is distributed into classes in different ways
 610 (the phytoplankton community structure changes). We can see that if we did not resolve the four classes, we could
 611 still use the Platt *et al.* (1980) model (including photoinhibition) for the total phytoplankton, but the parameters
 612 P_m^M, A_{13} , and A_{14} would vary depending on the (unresolved) variations in the phytoplankton community structure.
 613

614 5. A way forward

615 Together, these considerations suggest that investigating parameter assignment and parameter variability may be
 616 an important route to understand and potentially reduce many of the apparent differences between marine PP
 617 models, and hence in the estimated magnitudes of production. Investigation into the role of parameters should be
 618 followed by a consistent calibration against observational data. To estimate spatially and temporally varying
 619 parameters in ecosystem models, data assimilation can provide a natural tool for model calibration (e.g., Tjiputra
 620 *et al.*, 2007; Singh *et al.*, 2025). However, introducing spatio-temporally variable (or too many constant)
 621 parameters comes with its own challenges. For example, allowing the (often many) model parameters to vary
 622 substantially increases model flexibility, but at the risk of overfitting to observations, particularly if the number
 623 of model parameters is large or observational data are insufficient. Overfitting may reduce the model ability in
 624 predicting new phenomena, including future climate-driven changes. It is therefore essential that the introduction
 625 of variable parameters takes into account such risks and ensures that reasonable assumptions are made to simplify
 626 the parameter calibration task. These assumptions would ensure that model calibration is sufficiently constrained,
 627 so that there are sufficient observations per each calibrated model parameter value. For example, only a carefully
 628 selected subset of parameters may be calibrated, based on their relevance for PP (established, for example, through
 629 sensitivity analysis, e.g., Ciavatta *et al.*, 2025) and lack of correlations with other model parameters.

630 A key consideration when exploring variable parameters is the spatial and temporal scales at which they
631 might vary. For example, it would be important to establish whether seasonal, climatological variability in
632 parameters would be sufficient to capture observed patterns, implying that variability at shorter (sub-seasonal)
633 and longer (inter-annual) time scales could be negligible. If so, this would relax the requirement on the volumes
634 of observational data needed for the calibration, and also on the need to continually update parameter values from
635 day to day or year to year. Hypotheses about temporal variability scales for model parameters can be tested using
636 long time-series of measurements at specific stations, such as the Bermuda Atlantic Time-series Study and the
637 Hawaii Ocean Time-series, both of which present seasonal cycles in photosynthesis parameters (Kovač *et al.*,
638 2016b; Kovač *et al.*, 2018). Another key question is whether parameters vary over fine spatial scales or maintain
639 coherence over large scales such as within ocean biomes or Longhurst provinces (Longhurst, 2007). Preliminary
640 evidence suggests that, at least for the global-scale applications, ecological provinces according to Longhurst
641 might provide an appropriate template for mapping parameters (see Figure 6B), and that monthly or seasonal time
642 scales might be appropriate for modelling variability in photosynthesis-irradiance parameters (Britten *et al.*, 2025).
643 If province-based approaches emerge as viable candidates, it would be desirable to avoid sharp discontinuities in
644 parameter values at province boundaries, which might require incorporation of smoothing methods to make inter-
645 province changes seamless. Moreover, it is essential that model parameter calibration does not compensate for
646 unrelated spatio-temporally varying model biases, such as those arising from external forcings or other ecosystem
647 model constraints (e.g., boundary conditions). For example, given the importance of underlying physical
648 processes, caution should be applied when calibrating parameters in ecosystem models to avoid models better
649 reproducing the observed PP, but for the wrong reasons. Singh *et al.* (2025) illustrate that ecosystem parameters
650 in global ocean biogeochemical models are likely calibrated to compensate for biases in their physics (see also
651 Loptien and Dietze, 2019). To avoid mixing different sources of ecosystem model errors, parameters should be
652 ideally estimated jointly with the model state, e.g., using joint parameter-state data assimilation techniques
653 (Schartau *et al.*, 2017). Finally, existing knowledge of acceptable ranges of parameter values needs to be
654 incorporated into the calibration process to prevent parameters from acquiring unrealistic values.

655 Since parameter spatio-temporal variability results from poorly resolved species types or ecosystem
656 processes, interesting insights into its scale and patterns can be also obtained by comparing models of different
657 complexity. For example, high-complexity ecosystem models (such as the DARWIN ecosystem model) could be
658 used in some cases to deduce the degree of parameter variability of simpler ecosystem models or help inform
659 spatio-temporally varying parameter calibration of those models (always keeping in mind that inter-model
660 consistency does not automatically imply model quality). Comparison studies across models of different
661 complexity would be desirable in this case (for some examples see Friedrichs *et al.*, 2007; Xiao and Friedrichs,
662 2014). Similarly, emergent properties of ecosystem models can be leveraged to provide specific information for
663 satellite-based models, such as vertical and class-distribution of phytoplankton (e.g., Stock, 2019), or information
664 about nutrient distributions. Such inter-calibrations of models against each other could potentially improve
665 satellite PP products and conversely make the satellite PP data more useful for ecosystem model development.
666 However, one has to be cautious here: model-model intercomparisons and tuning would help models look more
667 like each other, but independent information would be needed to ensure that the simulations are also getting closer
668 to key features in the real world that the models are designed to reproduce.

669 Even after successfully overcoming the challenges associated with spatio-temporal parameter calibration,

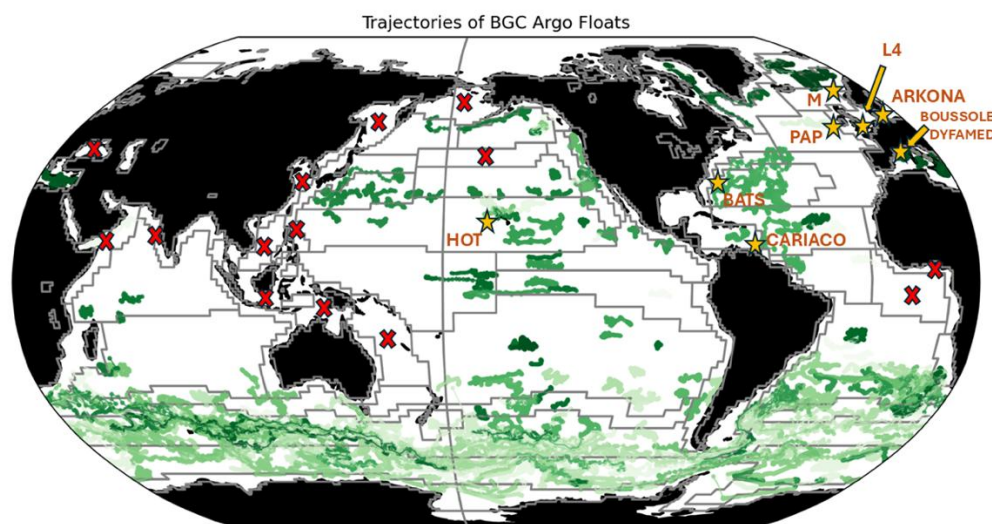
670 significant PP uncertainty is likely to remain in both historical estimates and future projections. For satellite-based
671 models, residual uncertainties could be associated with inherent observational biases, e.g., gaps in data due to
672 cloud cover or adverse viewing geometry, or inaccuracies in satellite products associated with bio-optical
673 conditions in water, or biases inherited from calibration against *in situ* PP observations with their own inherent
674 uncertainties. For ecosystem models, additional sources of uncertainty include the forcing data and the physical
675 model driving biogeochemical processes, e.g., its vertical and horizontal resolution, and its ability to represent
676 currents and mixing responsible for nutrient supply and export of organic material. For example, differences in
677 how models treat external forcing, such as micro- and macronutrient depositions from the atmosphere, could still
678 contribute to the growth of uncertainties as models become more complex. Furthermore, the spread in the
679 underlying environmental changes such as warming, stratification, changes in irradiation, and ocean circulation
680 among others, contributes significantly to uncertainties in the PP projection.

681 Further constraints are inherent to ecosystem models themselves. Traditionally, plankton are divided into
682 phototrophic phytoplankton and phagotrophic zooplankton. However, recent research emphasises ubiquitous
683 presence of mixotrophy in the global ocean (Mitra *et al.*, 2023), which not only differs in its physiology and
684 ecological role, but also in its complex interactions with other types of plankton (Flynn and Mitra, 2023). Despite
685 certain commonality in their approach to modelling PP, as discussed above, models differ significantly in their
686 approaches to representing various biogeochemical processes such as grazing and associated fluxes, deposition of
687 organic matter and its remineralisation. For many of those processes (e.g., zooplankton grazing), lack of data, and
688 variability and high uncertainty of available data, are major issues. Focusing on biological ocean carbon storage,
689 Henson *et al.* (2024) identified key areas where improved understanding of processes is required to support future
690 modelling efforts. For PP, the processes that were ranked highest were: resource limitation for growth, nitrogen
691 fixation, zooplankton processes and phytoplankton loss processes. Current ecosystem models differ considerably
692 in their formulation and parameterisation of these processes, contributing to uncertainties in model outcomes.
693 Moreover, nitrogen-fixation is often not included in these models. Even when these key processes are included,
694 spatial parameter estimation through assimilating observed state variables (such as water column nutrients and
695 oxygen) in ocean biogeochemical models does not necessarily lead to an improved estimate of PP, suggesting that
696 current ecosystem model parameterisations may still be oversimplified compared with the real world (Singh *et al.*,
697 2025).

698 The time is right to address the problem of parameter estimation in PP models, both for ecosystem models
699 and satellite-based models. Novel and rapidly expanding observations such as BGC Argo profiles, other types of
700 autonomous data collected by in-water vehicles and also large marine mammals (Chai *et al.*, 2020; Claustre *et al.*,
701 2020) have been providing large volumes of biological and bio-optical data that complements *in situ* data from
702 long time series stations, and could be harnessed for this purpose (Figure 10). Complementary observations from
703 satellite remote sensing, now available over multiple decades and merged into climate-quality, consistent data
704 streams (e.g., Sathyendranath *et al.*, 2019), is another rich data source, along with novel satellite products from
705 emerging capabilities such as geostationary, lidar, cubesat and hyperspectral data. When these are combined with
706 more traditional *in situ* platforms, including long-term gridded climatology from sources such as World Ocean
707 Atlas (WOA, e.g., Garcia *et al.*), and potentially complemented by the intercomparison of models with different
708 complexity, there is in several cases already enough data to support a suitably-constrained spatio-temporally
709 varying parameter calibration. This opportunity is further enhanced by new advances in artificial intelligence (AI)

710 and machine learning (ML), giving us an historically unprecedented capability to exploit large and growing
711 datasets to address long-standing questions about marine PP. AI can be used in a variety of different ways, either
712 as a direct prediction approach to optimise model parameterisation and also to emulate models, allowing it to
713 explore a range of model behaviours at reduced computational cost for parameter sensitivity analyses and model
714 calibration (e.g., Mattern *et al.*, 2012; Schartau *et al.*, 2017). Furthermore, recent statistical approaches unique to
715 the ML field enable insights into what the ML model has learned, for example, using Explainable AI, or physically
716 constrained machine learning.

717 However, crucial to this endeavour would be a clear focus on data quality, and on data validation, following
718 community-wide accepted protocols and reliable uncertainty characterisation. Moreover, some regions, such as
719 sea-ice margins, coastal margins, and high latitudes in winter, which are often regions experiencing long-term
720 rapid changes and include some of the most productive areas of the global ocean, also tend to be regions that are
721 difficult to observe, and hence suffer from sparse data coverage. More observations are needed in such locations
722 to understand the behaviour of model parameters in such regions, including their future changes. Even if
723 constrained spatio-temporally varying calibration is possible in these regions with the available datasets, the
724 importance of further investing in data quantity and quality cannot be overemphasised.



725
726 **Figure 10.** The global in situ data available for model calibration. The boundaries show ecological provinces
727 according to Longhurst (2007). BGC-Argo float trajectories are shown in shades of green, providing sufficiently
728 long time-series (since 2008) for calibration. Orange stars mark in situ time series stations with sufficiently long
729 time-series records that can also be used for model calibration. The red crosses mark provinces without sufficient
730 BGC-Argo data or in situ stations, where the models will need to rely solely on satellite records and compilations
731 of in situ observations, such as the World Ocean Atlas.

732

733 6. Conclusions

734 We have argued that, given the growing abundance of observations from diverse platforms, such as satellites and
735 BGC-Argo, combined with rapidly advancing capabilities in ensemble data assimilation techniques and artificial
736 intelligence, the time has now come to address explicitly the importance of parameter assignment in primary
737 production models, and in exploring the spatial and temporal variability in the parameters. We have theoretically
738 justified why such parameter variability is to be expected both in the satellite-based models (where some models

739 already employ variable parameters albeit in a simple fashion) and ecosystem models (where assignment of
740 variable parameters is still quite rare), at least in models are of high complexity. In the case of primary production,
741 the number of phytoplankton classes that are included in the model is a key differentiator of the model complexity.
742 Relatively simpler models, such as the ecosystem models used as part of ESMs in climate projections, have limited
743 capability to resolve phytoplankton communities. For such models, spatio-temporally varying parameters could
744 provide a means to account for the unresolved phytoplankton variability and processes.

745 Spatio-temporally variable parameter calibration can shed light on the sources of differences between low
746 or medium complexity ecosystem models typically used in ESMs and satellite-based primary-production models.
747 Since variable parameters can capture, in a simple manner, processes or conditions that are not explicitly included
748 in a model, analysing the drivers of parameter variability could help identify how best to overcome current model
749 drawbacks. Furthermore, providing those models with spatio-temporally varying parameters could remove many
750 apparent differences between models, both potentially reducing the spatial and temporal biases in model parameter
751 calibration and enabling the simpler ecosystem models to better represent the effects of unresolved processes or
752 phytoplankton classes. It would also create opportunities for improved intercomparison across models of different
753 complexity, including the ability to understand more about unresolved variability in simpler models by comparing
754 them with the higher-complexity models. One could argue that the spatio-temporally varying parametrisation
755 could help reduce the existing high uncertainty both in historical estimates and future projections of marine PP,
756 provided that independent information is used to avoid all models converging towards a systematically biased
757 outcome. Due to the importance of primary production for climate research, improving its prediction can have a
758 major impact on both climate mitigation and adaptation planning.

759 In the context of our climate, we need to understand how marine ecosystems in general, and phytoplankton
760 in particular, respond to change. Three types of changes need investigation: changes in (i) phytoplankton biomass
761 (whether they be measured as chlorophyll-a, carbon or nitrogen concentration, or all of them); (ii) the rates of
762 biological processes, with marine primary production being a key process in the global carbon cycle; and (iii)
763 community structure. All these objectives are intimately linked to parameter variability, with the third one in
764 particular calling for resolution of parameter variability at the level of major components of the phytoplankton
765 community.

766 For many decades, we have relied on comparisons and analyses of (both satellite and ecosystem) model
767 outputs with each other, and with *in situ* data, for insights into model performance, and for identifying the way
768 forward. It is now time to shift the emphasis toward understanding the behaviour of model parameters, across
769 models, across multiple phytoplankton types, and across multiple spatial and temporal scales. This focus has the
770 potential to reduce uncertainties, unify divergent model results, and provide a stronger foundation for predicting
771 marine primary production under changing climatic conditions.

772 **Code/data availability:** No new data, or code published in this paper.

773 **Author contributions:** JS organized the writing of the manuscript with substantial input by SS, and all the
774 authors contributed ideas, text and Figures.

775 **Competing interests:** The authors declare that they have no conflict of interest.

776

777 **Acknowledgments:** This work was funded by the European Space Agency (ESA) project Climate and Marine
778 Production (CAMP). JS, YA, GL, DB also acknowledge UK National Capability funding Atlantic Climate and
779 Environment Strategic Science (Atlantis). RJWB was supported by a UK Research and Innovation Future Leader
780 Fellowship (MR/V022792/1). SD acknowledges the Simons Collaboration on Computational Biogeochemical
781 Modelling of Marine Ecosystem (CBIOMES) (549931). BJ was supported by NASA (80NSSC21K0563,
782 Lagrangian analyses of ocean color and 80LARC21DA002 – GLIMR). ZK and MBK were supported in part by
783 the Croatian Science Foundation under the project number IP-2022-10-8859. FM thanks NERC for its support
784 (NE/X001261/1), RS is funded by the UKRI-NERC TerraFIRMA (NE/W004895/1) project, OU was supported
785 by a Royal Society Wolfson Visiting Fellowship (grant RSWVF\R3\223016), JT acknowledges the European
786 Union's Horizon 2020 (grant no. 817578), the European Union under grant agreement no. 101083922 (OceanICU)
787 and UK Research and Innovation (UKRI) under the UK government's Horizon Europe funding guarantee (grant
788 numbers 10054454, 10063673, 10064020, 10059241, 10079684, 10059012, 10048179).

789

790 **References**

791 Amirian, M. M., Finkel, Z. V., Devred, E., Irwin, A. J. (accepted). Parametrization of Photoinhibition for
792 Phytoplankton. *Communications Earth and Environment*.

793

794 Anderson, S.I., A.D. Barton, S. Clayton, S. Dutkiewicz, and T. Rynearson, 2021. Marine phytoplankton functional
795 types exhibit diverse responses to thermal change. *Nature Communications*, doi:10.1038/s41467-021-26651

796

797 Antoine D, Andre J-M, Morel A (1996). Oceanic primary production: 2. Estimation at global scale from satellite
798 (Coastal Zone Color Scanner) chlorophyll. *Global Biogeochemical Cycles*, 10:57-69.
799 <https://doi.org/10.1029/95GB02832>

800

801 Arteaga, L.A., Behrenfeld, M.J., Boss, E. and Westberry, T.K., 2022. Vertical structure in phytoplankton growth
802 and productivity inferred from biogeochemical-Argo floats and the carbon-based productivity model. *Global*
803 *Biogeochemical Cycles*, 36(8), p.e2022GB007389.

804

805 Behrenfeld, M.J. and Falkowski, P.G. (1997) Photosynthetic Rates Derived from Satellite-based Chlorophyll
806 Concentration. *Limnology and Oceanography*, 42, 1-20. <https://doi.org/10.4319/lo.1997.42.1.0001>

807

808 Behrenfeld MJ, Boss E, Siegel D, and Shea DM (2005) Carbon-based ocean productivity and phytoplankton
809 physiology from space. *Global Biogeochemical Cycles* 19. <https://doi.org/10.1029/2004GB002299>.

810

811 Bergas-Masso, E., Hamilton, D.S., Myriokefalitakis, S., Rathod, S., Gonçalves Ageitos, M. and Pérez García-
812 Pando, C., 2025. Future climate-driven fires may boost ocean productivity in the iron-limited North
813 Atlantic. *Nature Climate Change*, pp.1-9.

814

815 Blackford, J. C., Allen, J. I., and Gilbert, F. J.: Ecosystem dynamics at six contrasting sites: a generic modelling
816 study, *J. Marine Syst.*, 52, 191–215, 2004

817

818 Bopp, L., Resplandy, L., Orr, J. C., Doney, S. C., Dunne, J. P., Gehlen, M., Halloran, P., Heinze, C., Ilyina, T.,
819 Séférian, R., Tjiputra, J., and Vichi, M.: Multiple stressors of ocean ecosystems in the 21st century: projections
820 with CMIP5 models, *Biogeosciences*, 10, 6225–6245, <https://doi.org/10.5194/bg-10-6225-2013>, 2013.

821

822 Bopp, L., Aumont, O., Kwiatkowski, L., Clerc, C., Dupont, L., Ethé, C., Gorgues, T., Sférian, R., and Tagliabue,
823 A.: Diazotrophy as a key driver of the response of marine net primary productivity to climate change,
824 *Biogeosciences*, 19, 4267–4285, <https://doi.org/10.5194/bg-19-4267-2022>, 2022

825

826 Bouman, H.A., Platt, T., Doblin, M., Figueiras, M.G., Gudmundsson, K., Gudfinnsson, H.G., Huang, B.,
827 Hickman, A., Hiscock, M., Jackson, T., Lutz, V.A., Mélin, F., Rey, F., Pepin, P., Segura, V., Tilstone, G.H., van
828 Dongen-Vogels, V., Sathyendranath, S. (2018) Photosynthesis–irradiance parameters of marine phytoplankton:
829 synthesis of a global data set. *Earth Syst. Sci. Data*, 10: 251–266. <https://doi.org/10.5194/essd-10-251-2018>

830

831 RJW Brewin, GH Tilstone, T Jackson, T Cain, PI Miller (2017) Modelling size-fractionated primary production
832 in the Atlantic Ocean from remote sensing. *Progress in Oceanography*. 158: 130-149, ISSN 0079-6611,
833 <https://doi.org/10.1016/j.pocean.2017.02.002>.

834

835 Brewin, R.J., Sathyendranath, S., Kulk, G., Rio, M.H., Concha, J.A., Bell, T.G., Bracher, A., Fichot, C., Frölicher,
836 T.L., Galí, M. and Hansell, D.A., 2023. Ocean carbon from space: Current status and priorities for the next
837 decade. *Earth-science reviews*, 240, p.104386.

838

839 Butenschön, M., Clark, J., Aldridge, J.N., Allen, J.I., Artioli, Y., Blackford, J., Bruggeman, J., Cazenave, P.,
840 Ciavatta, S., Kay, S., Lessin, G. *et al.*, 2016. ERSEM 15.06: a generic model for marine biogeochemistry and the
841 ecosystem dynamics of the lower trophic levels. *Geoscientific Model Development*, 9(4), pp.1293-1339.

842

843 Carr, M.E., Friedrichs, M.A., Schmeltz, M., Aita, M.N., Antoine, D., Arrigo, K.R., Asanuma, I., Aumont, O.,
844 Barber, R., Behrenfeld, M. and Bidigare, R., 2006. A comparison of global estimates of marine primary production
845 from ocean color. *Deep Sea Research Part II: Topical Studies in Oceanography*, 53(5-7), pp.741-770.

846

847 Chai, F., Johnson, K.S., Claustre, H., Xing, X., Wang, Y., Boss, E., Riser, S., Fennel, K., Schofield, O. and Sutton,
848 A., 2020. Monitoring ocean biogeochemistry with autonomous platforms. *Nature Reviews Earth &*
849 *Environment*, 1(6), pp.315-326.

850

851 Ciavatta, S., Lazzari, P., Álvarez, E., Bertino, L., Bolding, K., Bruggeman, J., Capet, A., Cossarini, G., Daryabor,
852 F., Nerger, L., Popov, M. *et al.*, 2025. Control of simulated ocean ecosystem indicators by biogeochemical
853 observations. *Progress in Oceanography*, 231, p.103384.

854

855 Claustre, H, and Johnson, KS, and Takeshita, Y (2020) Observing the Global Ocean with Biogeochemical-Argo.
856 *Annual Review of Marine Science*,12: 23-48. <https://doi.org/10.1146/annurev-marine-010419-010956>

857

858 Daewel, U. and Schrum, C., 2013. Simulating long-term dynamics of the coupled North Sea and Baltic Sea
859 ecosystem with ECOSMO II: Model description and validation. *Journal of Marine Systems*, 119, pp.30-49.

860

861 Dai, R., Wen, Z., Hong, H., Browning, T.J., Hu, X., Chen, Z., Liu, X., Dai, M., Morel, F.M. and Shi, D., 2025.
862 Eukaryotic phytoplankton drive a decrease in primary production in response to elevated CO₂ in the tropical and
863 subtropical oceans. *Proceedings of the National Academy of Sciences*, 122(11), p.e2423680122.
864

865 Doléac, S., Lévy, M., El Hourany, R., and Bopp, L.: Toward more robust net primary production projections in
866 the North Atlantic Ocean, *Biogeosciences*, 22, 841–862, <https://doi.org/10.5194/bg-22-841-2025>, 2025.
867

868 Doney, S., Bopp, L., Long, M (2014) Historical and Future Trends in Ocean Climate and Biogeochemistry.
869 *Oceanography*. 27 (1), pp.108-119. [ff10.5670/oceanog.2014.14ff](https://doi.org/10.5670/oceanog.2014.14ff). [ffhal-03211060f](https://doi.org/10.1002/ffhal-03211060f)
870

871 Doron M, Brasseur P, Brankart JM, Losa SN, Melet A. Stochastic estimation of biogeochemical parameters from
872 Globcolour ocean colour satellite data in a North Atlantic 3D ocean coupled physical–biogeochemical model.
873 *Journal of Marine Systems*. 2013 May 1;117:81-95.
874

875 Droop, M. R.: The nutrient status of alga cells in continuous culture, *J. Mar. Biol. Assoc. UK*, 54, 825–855,
876 [doi:10.1016/0924-7963\(94\)00031-6](https://doi.org/10.1016/0924-7963(94)00031-6), 1974
877

878 Dutkiewicz, S., J.R. Scott, and M.J. Follows, 2013, Winners and Losers: Ecological and Biogeochemical Changes
879 in a Warming Ocean. *Global Biogeochemical Cycles*, 27, 463-477, [doi: 10.1002/gbc.20042](https://doi.org/10.1002/gbc.20042)
880

881 Dutkiewicz, S., Hickman, A.E., Jahn, O., Gregg, W.W., Mouw, C.B. and Follows, M.J., 2015. Capturing optically
882 important constituents and properties in a marine biogeochemical and ecosystem model. *Biogeosciences*, 12(14),
883 pp.4447-4481.
884

885 Dutkiewicz, S., Cermeno, P., Jahn, O., Follows, M.J., Hickman, A.E., Taniguchi, D.A. and Ward, B.A., 2020.
886 Dimensions of marine phytoplankton diversity. *Biogeosciences*, 17(3), pp.609-634.
887

888 Eppley, R., 1972. Temperature and phytoplankton growth in the sea. *Fishery bulletin*, 70(4), p.1063
889

890 Fasham, MJR, Ducklow, HW, McKelvie, SM (1990) A nitrogen-based model of plankton dynamics in the oceanic
891 mixed layer. *Journal of Marine Research*, 48: 591-639.
892

893 Fennel, K., Gehlen, M., Brasseur, P., Brown, C.W., Ciavatta, S., Cossarini, G., Crise, A., Edwards, C.A., Ford,
894 D., Friedrichs, M.A. and Gregoire, M., 2019. Advancing marine biogeochemical and ecosystem reanalyses and
895 forecasts as tools for monitoring and managing ecosystem health. *Frontiers in Marine Science*, 6, p.89.
896

897 Fennel, K., Mattern, J.P., Doney, S.C., Bopp, L., Moore, A.M., Wang, B. and Yu, L., 2022. Ocean biogeochemical
898 modelling. *Nature Reviews Methods Primers*, 2(1), p.76.
899

900 Field, CB, Behrenfeld, MJ, Randerson, JT, Falkowski, P (1998) Primary Production of the Biosphere: Integrating
901 terrestrial and oceanic Components. *Science* 281, 237-240. DOI: 10.1126/science.281.5374.237
902

903 Flynn, K.J. and Mitra, A., 2023. Feeding in mixoplankton enhances phototrophy increasing bloom-induced pH
904 changes with ocean acidification. *Journal of Plankton Research*, 45(4), pp.636-651.
905

906 Franks, P.J.S., 2002. NPZ models of plankton dynamics: their construction, coupling to physics, and application.
907 *J. Oceanogr.* 58, 379–387. DOI: 10.1023/a:1015874028196.
908

909 Friedlingstein, P., O'Sullivan, M., Jones, M. W., Andrew, R. M., Bakker, D. C. E., Hauck, J., Landschützer, P.,
910 Le Quéré, C., Lujckx, I. T., Peters, G. P., Peters, W., Pongratz, J., Schwingshackl, C., Sitch, S., Canadell, J. G.,
911 Ciais, P., Jackson, R. B., Alin, S. R., Anthoni, P., Barbero, L., Bates, N. R., Becker, M., Bellouin, N., Decharme,
912 B., Bopp, L., Brasika, I. B. M., Cadule, P., Chamberlain, M. A., Chandra, N., Chau, T.-T.-T., Chevallier, F., Chini,
913 L. P., Cronin, M., Dou, X., Enyo, K., Evans, W., Falk, S., Feely, R. A., Feng, L., Ford, D. J., Gasser, T., Ghattas,
914 J., Gkritzalis, T., Grassi, G., Gregor, L., Gruber, N., Gürses, Ö., Harris, I., Hefner, M., Heinke, J., Houghton, R.
915 A., Hurtt, G. C., Iida, Y., Ilyina, T., Jacobson, A. R., Jain, A., Jarníková, T., Jersild, A., Jiang, F., Jin, Z., Joos, F.,
916 Kato, E., Keeling, R. F., Kennedy, D., Klein Goldewijk, K., Knauer, J., Korsbakken, J. I., Körtzinger, A., Lan,
917 X., Lefèvre, N., Li, H., Liu, J., Liu, Z., Ma, L., Marland, G., Mayot, N., McGuire, P. C., McKinley, G. A., Meyer,
918 G., Morgan, E. J., Munro, D. R., Nakaoka, S.-I., Niwa, Y., O'Brien, K. M., Olsen, A., Omar, A. M., Ono, T.,
919 Paulsen, M., Pierrot, D., Pocock, K., Poulter, B., Powis, C. M., Rehder, G., Resplandy, L., Robertson, E.,
920 Rödenbeck, C., Rosan, T. M., Schwinger, J., Séférian, R., Smallman, T. L., Smith, S. M., Sospedra-Alfonso, R.,
921 Sun, Q., Sutton, A. J., Sweeney, C., Takao, S., Tans, P. P., Tian, H., Tilbrook, B., Tsujino, H., Tubiello, F., van
922 der Werf, G. R., van Ooijen, E., Wanninkhof, R., Watanabe, M., Wimart-Rousseau, C., Yang, D., Yang, X., Yuan,
923 W., Yue, X., Zaehle, S., Zeng, J., and Zheng, B.: Global Carbon Budget 2023, *Earth Syst. Sci. Data*, 15, 5301–
924 5369, <https://doi.org/10.5194/essd-15-5301-2023>, 2023.
925

926 Friedlingstein, P., O'sullivan, M., Jones, M.W., Andrew, R.M., Hauck, J., Landschützer, P., Le Quéré, C., Li, H.,
927 Lujckx, I.T., Olsen, A. and Peters, G.P., 2024. Global carbon budget 2024. *Earth System Science Data*
928 *Discussions*, 2024, pp.1-133.
929

930 Friedrichs, M.A., Dusenberry, J.A., Anderson, L.A., Armstrong, R.A., Chai, F., Christian, J.R., Doney, S.C.,
931 Dunne, J., Fujii, M., Hood, R. and McGillicuddy Jr, D.J., 2007. Assessment of skill and portability in regional
932 marine biogeochemical models: Role of multiple planktonic groups. *Journal of Geophysical Research: Oceans*,
933 112(C8).
934

935 Friedrichs, M.A.M., Carr, M.-E., Barber, R.T., Scardi, M., Antoine, D., Armstrong, R. A., *et al.* (2009) Assessing
936 the uncertainties of model estimates of primary productivity in the tropical Pacific Ocean. *J. Mar. Syst.* 76, 113-
937 133. doi:10.1016/j.jmarsys.2008.05.010
938

939 Frölicher, T. L., K. B. Rodgers, C. A. Stock, and W. W. L. Cheung (2016), Sources of uncertainties in 21st century
940 projections of potential ocean ecosystem stressors, *Global Biogeochem. Cycles*, 30, 1224–1243,
941 doi:10.1002/2015GB005338.

942

943 Galli, G., Wakelin, S., Harle, J., Holt, J., Artioli, Y., 2024. Multi-model comparison of trends and controls of near-
944 bed oxygen concentration on the northwest European continental shelf under climate change. *Biogeosciences* 21,
945 2143–2158. <https://doi.org/10.5194/bg-21-2143-2024>

946

947 Garcia, H.E., Weathers, K.W., Paver, C.R., Smolyar, I., Boyer, T.P., Locarnini, M.M., Zweng, M.M., Mishonov,
948 A.V., Baranova, O.K. and Seidov, D., 2019. World ocean atlas 2018. Vol. 4: Dissolved inorganic nutrients
949 (phosphate, nitrate and nitrate+ nitrite, silicate).

950

951 Gastineau, G., & Soden, B. J. (2009). Model projected changes of extreme wind events in response to global
952 warming. *Geophysical Research Letters*, 36(10). <https://doi.org/10.1029/2009GL037500>

953

954 Gattuso, J.P., Frankignoulle, M. and Wollast, R., 1998. Carbon and carbonate metabolism in coastal aquatic
955 ecosystems. *Annual Review of Ecology and Systematics*, 29(1), pp.405-434.

956

957 Geider, RJ, Macintyre, HL, and Kana, TM (1997) Dynamic model of phytoplankton growth and acclimation:
958 responses of the balanced growth rate and the chlorophyll a: carbon ratio to light, nutrient imitation and
959 temperature,” *Mar. Ecol. Prog. Ser.* 148, 187–200.

960

961 Geider RJ, MacIntyre HL, Kana TM. (1998) A dynamic regulatory model of phytoplankton acclimation to light,
962 nutrients, and temperatures. *Limnol. Oceanogr.*, 43(4), 679-694.

963

964 Gentile, E. S., Zhao, M., & Hodges, K. (2023). Poleward intensification of midlatitude extreme winds under
965 warmer climate. *Npj Climate and Atmospheric Science*, 6(1), 1–10. <https://doi.org/10.1038/s41612-023-00540-x>

966

967 Gentleman, W., 2002. A chronology of plankton dynamics in silico: how computer models have been used to
968 study marine ecosystems. *Hydrobiologia* 480, 69–85. DOI: 10.1023/A:1021289119442.

969

970 Gharamti ME, Samuelsen A, Bertino L, Simon E, Korosov A, Daewel U. Online tuning of ocean biogeochemical
971 model parameters using ensemble estimation techniques: Application to a one-dimensional model in the North
972 Atlantic. *Journal of Marine Systems*. 2017 Apr 1;168:1-6.

973

974 Gharamti ME, Tjiputra J, Bethke I, Samuelsen A, Skjelvan I, Bentsen M, Bertino L. Ensemble data assimilation
975 for ocean biogeochemical state and parameter estimation at different sites. *Ocean Modelling*. 2017 Apr 1;112:65-
976 89.

977

978 Gregg, W.W. and Rousseaux, C.S., 2016. Directional and spectral irradiance in ocean models: Effects on
979 simulated global phytoplankton, nutrients, and primary production. *Frontiers in Marine Science*, 3, p.240.
980

981 Gregg W.W and Rousseaux C.S. 2019. Global ocean primary production trends in the modern ocean color satellite
982 record (1998–2015). *Environ. Res. Lett.* 14 124011
983

984 Grégoire, M. and Soetaert, K., 2010. Carbon, nitrogen, oxygen and sulfide budgets in the Black Sea: A
985 biogeochemical model of the whole water column coupling the oxic and anoxic parts. *Ecological Modelling*,
986 221(19), pp.2287-2301.
987

988 Grégoire, M., Raick, C. and Soetaert, K., 2008. Numerical modeling of the central Black Sea ecosystem
989 functioning during the eutrophication phase. *Progress in Oceanography*, 76(3), pp.286-333.
990

991 Grégoire, M. and Soetaert, K., 2010. Carbon, nitrogen, oxygen and sulfide budgets in the Black Sea: A
992 biogeochemical model of the whole water column coupling the oxic and anoxic parts. *Ecological Modelling*,
993 221(19), pp.2287-2301.
994

995 Gulev, S.K., P.W. Thorne, J. Ahn, F.J. Dentener, C.M. Domingues, S. Gerland, D. Gong, D.S. Kaufman, H.C.
996 Nnamchi, J. Quaas, J.A. Rivera, S. Sathyendranath, S.L. Smith, B. Trewin, K. von Schuckmann, and R.S. Vose,
997 2021: Changing State of the Climate System. In *Climate Change 2021: The Physical Science Basis. Contribution*
998 *of Working Group I to the Sixth Assessment Report of the Intergovernmental Panel on Climate Change* [Masson-
999 Delmotte, V., P. Zhai, A. Pirani, S.L. Connors, C. Péan, S. Berger, N. Caud, Y. Chen, L. Goldfarb, M.I. Gomis,
1000 M. Huang, K. Leitzell, E. Lonnoy, J.B.R. Matthews, T.K. Maycock, T. Waterfield, O. Yelekçi, R. Yu, and B.
1001 Zhou (eds.)]. Cambridge University Press, Cambridge, United Kingdom and New York, NY, USA, pp. 287–422,
1002 doi: 10.1017/9781009157896.004.
1003

1004 Halsey, K.H., Milligan, A.J. and Behrenfeld, M.J., 2011. Linking time-dependent carbon-fixation efficiencies in
1005 *Dunaliella Tertiolecta* (Chlorophyceae) to underlying metabolic pathways 1. *Journal of Phycology*, 47(1), pp.66-
1006 76.
1007

1008 Henson, S., Baker, C.A., Halloran, P., McQuatters-Gollop, A., Painter, S., Planchat, A. and Tagliabue, A., 2024.
1009 Knowledge gaps in quantifying the climate change response of biological storage of carbon in the ocean. *Earth's*
1010 *Future*, 12(6), p.e2023EF004375.
1011

1012 Hewitt, C. D., and Coauthors, 2021: Recommendations for Future Research Priorities for Climate Modeling and
1013 Climate Services. *Bull. Amer. Meteor. Soc.*, 102, E578–E588, <https://doi.org/10.1175/BAMS-D-20-0103.1>.
1014

1015 IOCCG (2020). Synergy between Ocean Colour and Biogeochemical/Ecosystem Models. Dutkiewicz, S. (ed.),
1016 IOCCG Report Series, No. 19, International Ocean Colour Coordinating Group, Dartmouth, Canada.
1017 <http://dx.doi.org/10.25607/OBP-711>

1018

1019 IOCCG Protocol Series (2022). Aquatic Primary Productivity Field Protocols for Satellite Validation and Model
1020 Synthesis. Balch, W.M., Carranza, M., Cetinić, I., Chaves, J.E., Duhamel, S., Fassbender, A., Fernandez-Carrera,
1021 A., Ferrón, S., García-Martín, E., Goes, J., Gomes, H., Gundersen, K., Halsey, K., Hirawake, T., Isada, T., Juranek,
1022 L., Kulk, G., Langdon, C., Letelier, R., López-Sandoval, D., Mannino, A., Marra, J.F., Neale, P., Nicholson, D.,
1023 Silsbe, G., Stanley, R.H., Vandermeulen, R.A. IOCCG Ocean Optics and Biogeochemistry Protocols for Satellite
1024 Ocean Colour Sensor Validation, Volume 7.0, edited by R.A. Vandermeulen, J. E. Chaves, IOCCG, Dartmouth,
1025 NS, Canada. doi:<http://dx.doi.org/10.25607/OBP-1835>

1026

1027 IPCC (2019): IPCC Special Report on the Ocean and Cryosphere in a Changing Climate [H.-O. Pörtner, D.C.
1028 Roberts, V. Masson-Delmotte, P. Zhai, M. Tignor, E. Poloczanska, K. Mintenbeck, A. Alegria, M. Nicolai, A.
1029 Okem, J. Petzold, B. Rama, N.M. Weyer (eds.)].

1030

1031 IPCC, 2021: Climate Change 2021 - the Physical Science Basis, Contribution of Working Group I to the Sixth
1032 Assessment Report of the Intergovernmental Panel on Climate Change [Masson-Delmotte, V., P. Zhai, A. Pirani,
1033 S.L. Connors, C. Péan, S. Berger, N. Caud, Y. Chen, L. Goldfarb, M.I. Gomis, M. Huang, K. Leitzell, E. Lonnoy,
1034 J.B.R. Matthews, T.K. Maycock, T. Waterfield, O. Yelekçi, R. Yu, and B. Zhou (eds.)]. Cambridge University
1035 Press, In Press, Published: 9 August 2021.

1036

1037 Jackson, T, Sathyendranath, S, and T. Platt, T (2017) An exact solution for modeling photoacclimation of the
1038 carbon-to-chlorophyll ratio in phytoplankton, *Front. Mar. Sci.* 4, 283

1039

1040 Jassby, A.D. and Platt, T., 1976. Mathematical formulation of the relationship between photosynthesis and light
1041 for phytoplankton. *Limnology and oceanography*, 21(4), pp.540-547.

1042

1043 Jin, P., Hutchins, D.A. and Gao, K., 2020. The impacts of ocean acidification on marine food quality and its
1044 potential food chain consequences. *Frontiers in Marine Science*, 7, p.543979.

1045

1046 Jones, C. G., Adloff, F., Booth, B., Cox, P., Eyring, V., Friedlingstein, P., Frieler, K., Hewitt, H., Jeffery, H.,
1047 Jousaume, S., Koenigk, T., Lawrence, B. N., O'Rourke, E., Roberts, M., Sanderson, B., Séférian, R., Somot, S.,
1048 Vidale, P.-L., van Vuuren, D., Acosta, M., Bentsen, M., Bernardello, R., Betts, R., Blockley, E., Boé, J.,
1049 Bracegirdle, T., Braconnot, P., Brovkin, V., Buontempo, C., Doblus-Reyes, F. J., Donat, M. G., Epicoco, I.,
1050 Falloon, P., Fiore, S., Froelicher, T., Fuckar, N., Gidden, M., Goessling, H., Graverson, R. G., Gualdi, S.,
1051 Gutiérrez, J. M., Ilyina, T., Jacob, D., Jones, C., Juckes, M., Kendon, E., Kjellström, E., Knutti, R., Lowe, J. A.,
1052 Mizieliński, M., Nassisi, P., Obersteiner, M., Regnier, P., Roehrig, R., Salas y Melia, D., Schleussner, C.-F.,
1053 Schulz, M., Scoccimarro, E., Terray, L., Thiemann, H., Wood, R., Yang, S., and Zaehle, S.: Bringing it all
1054 together: Science and modelling priorities to support international climate policy, *EGUsphere* [preprint],
1055 <https://doi.org/10.5194/egusphere-2024-453>, 2024.

1056

1057 Kiefer, D.A. and Mitchell, B.G., 1983. A simple, steady state description of phytoplankton growth based on
1058 absorption cross section and quantum efficiency 1. *Limnology and Oceanography*, 28(4), pp.770-776.
1059

1060 Kim, H.H., Laufkötter, C., Lovato, T., Doney, S.C. and Ducklow, H.W., 2023. Projected 21st-century changes in
1061 marine heterotrophic bacteria under climate change. *Frontiers in microbiology*, 14, p.1049579.
1062

1063 Kishi, M.J., Kashiwai, M., Ware, D.M., Megrey, B.A., Eslinger, D.L., Werner, F.E., Noguchi-Aita, M., Azumaya,
1064 T., Fujii, M., Hashimoto, S. and Huang, D., 2007. NEMURO—a lower trophic level model for the North Pacific
1065 marine ecosystem. *Ecological Modelling*, 202(1-2), pp.12-25.
1066

1067 Kovač, Ž., Platt, T., Sathyendranath, S., Morović, M., Jackson, T. (2016a). Recovery of photosynthesis parameters
1068 from in situ profiles of phytoplankton production. *ICES Journal of Marine Science*, 73 (2), 275–285. DOI:
1069 10.1093/icesjms/fsv204.
1070

1071 Kovač, Ž., Platt, T., Sathyendranath, S., Morović, M. (2016b). Analytical solution for the vertical profile of daily
1072 production in the ocean. *Journal of Geophysical Research: Oceans*, 121. DOI: 10.1002/2015JC011293.
1073

1074 Kovač, Ž., Platt, T., S., S., Antunović, S. (2017). Models for estimating photosynthesis parameters from in situ
1075 production profiles. *Progress in Oceanography*, 159, 255-266. doi:10.1016/j.pocean.2017.10.013.
1076

1077 Kovač, Ž., Platt, T., Sathyendranath, S., Lomas, M. W. (2018). Extraction of photosynthesis parameters from time
1078 series measurements of in situ production: Bermuda atlantic time-series study. *Remote Sensing*, 10, 915. DOI:
1079 10.3390/rs10060915.
1080

1081 Kovárová-Kovar, K. and Egli, T., 1998. Growth kinetics of suspended microbial cells: from single-substrate-
1082 controlled growth to mixed-substrate kinetics. *Microbiology and molecular biology reviews*, 62(3), pp.646-666.
1083

1084 Krinos, A.I., Shapiro, S.K., Li, W., Haley, S.T., Dyhrman, S.T., Dutkiewicz, S., Follows, M.J. and Alexander, H.
1085 (2025), Intraspecific Diversity in Thermal Performance Determines Phytoplankton Ecological Niche. *Ecology*
1086 *Letters*, 28: e70055. <https://doi.org/10.1111/ele.70055>
1087

1088 Kulk, G, Platt, T, Dingle, J, Jackson, T, Jönsson, BF, Bouman, HA, Babin, M, Brewin, RJW, Doblin, M, Estrada,
1089 M, Figueiras, FG, Furuya, K, González-Benítez, N, Gudfinnsson, HG, Gudmundsson, K, Huang, B, Isada, T,
1090 Kovač, Ž, Lutz, VA, Marañón, E, Raman, M, Richardson, K, Rozema, PD, Poll, WH, Segura, V, Tilstone, GH,
1091 Uitz, J, Dongen-Vogels, V, Yoshikawa, T, Sathyendranath, S (2020) Primary Production, an Index of Climate
1092 Change in the Ocean: Satellite-Based Estimates over Two Decades. *Remote Sensing*, 12, 826.
1093 <https://doi.org/10.3390/rs12050826>
1094

1095 Kulk, G.; Platt, T.; Dingle, J.; Jackson, T.; Jönsson, B.F.; Bouman, H.A.; Babin, M.; Brewin, R.J.W.; Doblin, M.;
1096 Estrada, M.; *et al.* Correction: Kulk *et al.* Primary Production, an Index of Climate Change in the Ocean: Satellite-

1097 Based Estimates over Two Decades. *Remote Sens.* 2020, 12, 826. *Remote Sens.* 2021, 13, 3462.
1098 <https://doi.org/10.3390/rs13173462>
1099

1100 Kyewalyanga, M., Platt, T., & Sathyendranath, S. (1992). Ocean primary production calculated by spectral and
1101 broadband models. *Marine Ecology Progress Series*, 85, 171–185. DOI: 10.3354/meps085171.
1102

1103 Kyewalyanga, MN, Platt, T, Sathyendranath, S (1997) Estimation of the photosynthetic action spectrum:
1104 implications for primary production models. *Mar. Ecol. Prog. Ser.* 146: 207-223.
1105

1106 Kwiatkowski, L., Bopp, L., Aumont, O., Ciais, P., Cox, P.M., Laufkötter, C., Li, Y. and Séférian, R., 2017.
1107 Emergent constraints on projections of declining primary production in the tropical oceans. *Nature Climate*
1108 *Change*, 7(5), pp.355-358.
1109

1110 Kwiatkowski, L., Torres, O., Bopp, L., Aumont, O., Chamberlain, M., Christian, J.R., Dunne, J.P., Gehlen, M.,
1111 Ilyina, T., John, J.G., Lenton, A., Li, H., Lovenduski, N.S., Orr, J.C., Palmieri, J., Santana-Falcón, Y., Schwinger,
1112 J., Séférian, R., Stock, C.A., Tagliabue, A., Takano, Y., Tjiputra, J., Toyama, K., Tsujino, H., Watanabe, M.,
1113 Yamamoto, A., Yool, A., Ziehn, T., 2020. Twenty-first century ocean warming, acidification, deoxygenation, and
1114 upper-ocean nutrient and primary production decline from CMIP6 model projections. *Biogeosciences* 17, 3439–
1115 3470. <https://doi.org/10.5194/bg-17-3439-2020>
1116

1117 Laufkötter, C., Vogt, M., Gruber, N., Aita-Noguchi, M., Aumont, O., Bopp, L., Buitenhuis, E., Doney, S. C.,
1118 Dunne, J., Hashioka, T., Hauck, J., Hirata, T., John, J., Le Quére, C., Lima, I. D., Nakano, H., Seferian, R.,
1119 Totterdell, I., Vichi, M., and Völker, C. (2015) Drivers and uncertainties of future global marine primary
1120 production in marine ecosystem models, *Biogeosciences*, 12, 6955–6984, [https://doi.org/10.5194/bg-12-6955-](https://doi.org/10.5194/bg-12-6955-2015)
1121 2015
1122

1123 Lee, Z. Veronica P. Lance, VP, Shang, S, Vaillancourt,R, Freeman,S, Lubac, B, Hargreaves, BR, Del Castillo, C,
1124 Richard Miller, R, Twardowski, M, Wei, G (2011) An assessment of optical properties and primary production
1125 derived from remote sensing in the Southern Ocean (SO GasEx). *J. Geophys. Res.* 116, C00F03 (2011).
1126 doi:10.1029/2010JC006747.
1127

1128 Lee Z, Marra J, Perry MJ, Kahru M (2015). Estimating oceanic primary productivity from ocean color remote
1129 sensing: A strategic assessment, *Journal of Marine Systems*. <http://dx.doi.org/10.1016/j.jmarsys.2014.11.015>Lee,
1130 S. and Yoo, S. (2016) ‘Interannual variability of the phytoplankton community by the changes in vertical mixing
1131 and atmospheric deposition in the Ulleung Basin, East Sea: A modelling study’, *Ecological Modelling*, 322, pp.
1132 31–47. Available at: <https://doi.org/10.1016/j.ecolmodel.2015.11.012>.
1133

1134 Lee, Y. J., P. A. Matrai, M. A. M. Friedrichs, V. S. Saba, D. Antoine, M. Ardyna, I. Asanuma, M. Babin, S.
1135 Belanger, M. Benoit-Gagne, E. Devred, M. Fernandez-Mendez, B. Gentili, T. Hirawake, S.-H. Kang, T. Kameda,
1136 C. Katlein, S.H. Lee, Z. Lee, F. Melin, M. Scardi, T.J. Smyth, S. Tang, K.R. Turpie, K.J. Waters, and T.K.

1137 Westberry (2015). An assessment of ocean color model estimates of primary productivity in the Arctic Ocean. *J.*
1138 *Geophys. Res. Oceans*, FAMOS SI, 120:6508–6541, DOI 10.1002/2015JC011018.

1139

1140 Liu, H., Li, D., Chen, Q., Feng, J., Qi, J., & Yin, B. (2024). The multiscale variability of global extreme wind and
1141 wave events and their relationships with climate modes. *Ocean Engineering*, 307, 118239.
1142 <https://doi.org/10.1016/j.oceaneng.2024.118239>

1143

1144 Longhurst, A, Sathyendranath, S, Platt, T, Caverhill, C (1995) An estimate of global primary production in the
1145 ocean from satellite radiometer data. *J. Plankton Res.* 17: 1245-1271.

1146

1147 Longhurst, A.R. *Ecological Geography of the Sea*, 2nd ed.; Elsevier Academic Press: Cambridge, MA, USA,
1148 2007; p. 542.

1149

1150 Löptien, U. and Dietze, H., 2019. Reciprocal bias compensation and ensuing uncertainties in model-based climate
1151 projections: pelagic biogeochemistry versus ocean mixing. *Biogeosciences*, 16(9), pp.1865-1881.

1152

1153 Lurin, B., Rasool, S.I., Cramer, W. and Moore, B. (1994) Global terrestrial net primary production. *Glob. Change*
1154 *NewsL (IGBP)*, 19, 6-8.

1155

1156 Luypaert, T., Hagan, J.G., McCarthy, M.L. and Poti, M., 2020. Status of marine biodiversity in the
1157 Anthropocene. *YOUMARES*, 9, pp.57-82.

1158

1159 Maishal, S., 2024. Decadal changes in global Oceanic Primary Productivity and its drivers. *Ocean-Land-*
1160 *Atmosphere Research*, 3, p.0066.

1161

1162 Marshak, A.R., Link, J.S. Primary production ultimately limits fisheries economic performance. *Sci Rep* 11,
1163 12154 (2021). <https://doi.org/10.1038/s41598-021-91599-0>

1164

1165 Mattern J P., Fennel K., Dowd M. (2012). Estimating time-dependent parameters for a biological ocean model
1166 using an emulator approach. *J. Mar. Syst.* 96, 32–47. doi: 10.1016/j.jmarsys.2012.01.015.

1167 Michaelis L, Menten ML. Die kinetik der invertinwirkung. *Biochem. z.* 1913 Feb;49(333-369):352.

1168

1169 Mitra, A., Caron, D.A., Faure, E., Flynn, K.J., Leles, S.G., Hansen, P.J., McManus, G.B., Not, F., do Rosario
1170 Gomes, H., Santoferrara, L.F. and Stoecker, D.K., 2023. The Mixoplankton Database (MDB): Diversity of photo-
1171 phago-trophic plankton in form, function, and distribution across the global ocean. *Journal of Eukaryotic*
1172 *Microbiology*, 70(4), p.e12972.

1173

1174 Myksvoll, M.S., Sandø, A.B., Tjiputra, J., Samuelsen, A., Yumruktepe, V.Ç., Li, C., Mousing, E.A., Bettencourt,
1175 J.P. and Ottersen, G., 2023. Key physical processes and their model representation for projecting climate impacts
1176 on subarctic Atlantic net primary production: A synthesis. *Progress in Oceanography*, 217, p.103084.

1177
1178 Norberg J., Biodiversity and ecosystem functioning: A complex adaptive systems approach, *Limnology and*
1179 *Oceanography*, 4, part 2, doi: 10.4319/lo.2004.49.4_part_2.1269. 2004.
1180
1181 T. Parsons, M. Takahashi, B. Hargrave., *Biological Oceanographic Processes* (Third edition), Pergamon
1182 International Library of Science, Technology, Engin, Pergamon (1984)
1183
1184 Pastres, R., Ciavatta, S. and Solidoro, C., 2003. The Extended Kalman Filter (EKF) as a tool for the assimilation
1185 of high frequency water quality data. *Ecological modelling*, 170(2-3), pp.227-235.
1186
1187 Platt, T., Gallegos, C.L. and Harrison, W.G., 1980. Photoinhibition of photosynthesis in natural assemblages of
1188 marine phytoplankton.
1189
1190 Platt, T., Sathyendranath, S (1988) Oceanic primary production: Estimation by remote sensing at local and
1191 regional scales. *Science* 241: 1613-1620.
1192
1193 Platt, T., Sathyendranath, S, Ravindran, P (1990) Primary production by phytoplankton: analytic solutions for
1194 daily rates per unit area of water surface. *Proc. R. Soc. Lond. Ser. B* 241: 101-111.
1195
1196 Platt, T, Sathyendranath, S (1991) Biological production models as elements of coupled, atmosphere-ocean
1197 models for climate research. *J. Geophys. Res.* 96: 2585-2592.
1198
1199 Platt, T, Sathyendranath, S (1993) Estimators of primary production for interpretation of remotely sensed data on
1200 ocean color. *J. Geophys. Res.* 98: 14,561-14,576.
1201 Platt, T, Sathyendranath, S (1997) Modelling primary production IV (in Japanese). *Aquabiology* 19: 229-232.
1202
1203 Radtke, H., Lipka, M., Bunke, D., Morys, C., Woelfel, J., Cahill, B., Böttcher, M.E., Forster, S., Leipe, T., Rehder,
1204 G. and Neumann, T., 2019. Ecological ReGional Ocean Model with vertically resolved sediments (ERGOM SED
1205 1.0): coupling benthic and pelagic biogeochemistry of the south-western Baltic Sea. *Geoscientific Model*
1206 *Development*, 12(1), pp.275-320.
1207
1208 Ratnarajah L, Abu-Alhaja R, Atkinson A, Batten S, Bax NJ, Bernard KS, Canonico G, Cornils A, Everett JD,
1209 Grigoratou M, Ishak NH. Monitoring and modelling marine zooplankton in a changing climate. *Nature*
1210 *Communications*. 2023 Feb 2;14(1):564.
1211
1212 Regaudie-de-Gioux, A., Lasternas, S., Agustí, S., Duarte, C.M. 2019. Comparing marine primary production
1213 estimates through different methods and development of conversion equations. *Frontiers in Marine Science*, 1.
1214 URL: <https://www.frontiersin.org/journals/marine-science/articles/10.3389/fmars.2014.00019>. DOI=10.3389/
1215 fmars.2014.00019
1216

1217 Rohr T, Richardson AJ, Lenton A, Chamberlain MA, Shadwick EH. Zooplankton grazing is the largest source of
1218 uncertainty for marine carbon cycling in CMIP6 models. *Communications Earth & Environment*. 2023 Jun
1219 14;4(1):212.
1220

1221 Roy S, Broomhead DS, Platt T, Sathyendranath S, Ciavatta S. Sequential variations of phytoplankton growth and
1222 mortality in an NPZ model: A remote-sensing-based assessment. *Journal of Marine Systems*. 2012 Apr
1223 1;92(1):16-29.
1224

1225 Ryan-Keogh, T.J., Tagliabue, A. & Thomalla, S.J. Global decline in net primary production underestimated by
1226 climate models. *Commun Earth Environ* 6, 75 (2025). <https://doi.org/10.1038/s43247-025-02051-4>
1227

1228 Saba, V.S., Friedrichs, M.A.M., Carr, M.-E., Antoine, D., Armstrong, R.A., Asanuma, I., *et al.*(2010) Challenges
1229 of modeling depth-integrated marine primary productivity over multiple decades: a case study at BATS and HOT.
1230 *Glob. Biogeochem. Cycle* 24, GB3020.[doi:10.1029/2009GB003655](https://doi.org/10.1029/2009GB003655)
1231

1232 Sathyendranath, S., & Platt, T. (1989a). Computation of aquatic primary production: Extended formalism to
1233 include the effect of angular and spectral distribution of light. *Limnology and Oceanography*, 34, 188–198. DOI:
1234 10.4319/lo.1989.34.1.0188.
1235

1236 Sathyendranath, S, Platt, T, Caverhill, CM, Warnock, RE, Lewis, MR (1989b) Remote sensing of oceanic primary
1237 production: Computations using a spectral model. *Deep-Sea Res. I* 36: 431-453.
1238

1239 Sathyendranath, S, Platt, T (2007) Spectral effects in bio-optical control on the ocean system. *Oceanologia* 49: 5-
1240 39.
1241

1242 Sathyendranath, S, Stuart, V, Nair, A, Oka, K., Nakane, T, Bouman, H, Forget, M-H, Maass, H, Platt, T (2009)
1243 Carbon-to-chlorophyll ratio and growth rate of phytoplankton in the sea. *Mar. Ecol. Prog. Ser.* 383: 73–84, doi:
1244 10.3354/meps07998
1245

1246 Sathyendranath, S., Brewin, R., Brockmann, C., Brotas, V., Calton, B., Chuprin, A., *et al.* (2019). An ocean-
1247 colour time series for use in climate studies: The experience of the Ocean-Colour Climate Change Initiative (OC-
1248 CCI). *Sensors*, 19(19), 4285. <https://doi.org/10.3390/s19194285>
1249

1250 Sathyendranath, S, Platt, T, Kovač, Ž, Dingle, J, Jackson, T, Brewin, R JW, Franks, P, Marañón, E, Kulk, G, and
1251 Bouman, HA (2020) Reconciling models of primary production and photoacclimation [Invited]. *Applied Optics*,
1252 59: C100-C114. <https://doi.org/10.1364/AO.386252>
1253

1254 Sathyendranath, S., Brewin, R.J.W., Ciavatta, S. Jackson, T., Kulk, G., Jönsson, B. Martinez Vicente, V, Platt, T.
1255 (2023) Ocean Biology Studied from Space. *Surv Geophys* 44, 1287–1308. [https://doi.org/10.1007/s10712-023-](https://doi.org/10.1007/s10712-023-09805-9)
1256 [09805-9](https://doi.org/10.1007/s10712-023-09805-9)

1257

1258 Sauterey B., Le Gland G., Cermeño P., Aumont O., Lévy M., Vallina S.M., Phytoplankton adaptive resilience to
1259 climate change collapses in case of extreme events – A modeling study. *Ecological Modelling*, Volume 483, 2023,
1260 110437, ISSN 0304-3800, <https://doi.org/10.1016/-j.ecolmodel.2023.110437>

1261

1262 Séférian, R., Berthet, S., Yool, A., Palmiéri, J., Bopp, L., Tagliabue, A., Kwiatkowski, L., Aumont, O., Christian,
1263 J., Dunne, J., Gehlen, M., Ilyina, T., John, J.G., Li, H., Long, M.C., Luo, J.Y., Nakano, H., Romanou, A.,
1264 Schwinger, J., Stock, C., Santana-Falcón, Y., Takano, Y., Tjiputra, J., Tsujino, H., Watanabe, M., Wu, T., Wu,
1265 F., Yamamoto, A., 2020. Tracking Improvement in Simulated Marine Biogeochemistry Between CMIP5 and
1266 CMIP6. *Curr Clim Change Rep* 6, 95–119. <https://doi.org/10.1007/s40641-020-00160-0>

1267

1268 Schartau, M., Wallhead, P., Hemmings, J., Löptien, U., Kriest, I., Krishna, S., Ward, B. A., Slawig, T., and
1269 Oschlies, A.: Reviews and syntheses: parameter identification in marine planktonic ecosystem modelling,
1270 *Biogeosciences*, 14, 1647–1701, <https://doi.org/10.5194/bg-14-1647-2017>, 2017.

1271

1272 Schmidtko S., Stramma L., Visbeck M. (2017). Decline in global oceanic oxygen content during the past five
1273 decades. *Nature* 542, 335–339. doi: 10.1038/nature21399

1274

1275 Shigemitsu, M., Okunishi, T., Nishioka, J., Sumata, H., Hashioka, T., Aita, M.N., Smith, S.L., Yoshie, N., Okada,
1276 N. and Yamanaka, Y., 2012. Development of a one-dimensional ecosystem model including the iron cycle applied
1277 to the Oyashio region, western subarctic Pacific. *Journal of Geophysical Research: Oceans*, 117(C6).

1278

1279 Silsbe, G.M., Behrenfeld, M.J., Halsey, K.H., Milligan, A.J. and Westberry, T.K., 2016. The CAFE model: A net
1280 production model for global ocean phytoplankton. *Global Biogeochemical Cycles*, 30(12), pp.1756-1777.

1281

1282 Silsbe, G.M., Fox, J., Westberry, T.K. *et al.* Global declines in net primary production in the ocean color era. *Nat*
1283 *Commun* 16, 5821 (2025). <https://doi.org/10.1038/s41467-025-60906-y>

1284

1285 Simon E, Samuelsen A, Bertino L, Mouysset S. Experiences in multiyear combined state–parameter estimation
1286 with an ecosystem model of the North Atlantic and Arctic Oceans using the Ensemble Kalman Filter. *Journal of*
1287 *Marine Systems*. 2015 Dec 1;152:1-7.

1288

1289 Singh, T., Counillon, F., Tjiputra, J. and Wang, Y., 2025. A novel ensemble-based parameter estimation for
1290 improving ocean biogeochemistry in an Earth system model. *Journal of Advances in Modeling Earth*
1291 *Systems*, 17(2), p.e2024MS004237.

1292

1293 Skákala, J., Wakamatsu, T., Bertino, L., Teruzzi, A., Lazzari, P., Alvarez, E., Cossarini, G., Spada, S., Nerger, L.,
1294 Vliegen, S., Brankart, J. M., and Brasseur, P.: SEAMLESS Target indicator quality in CMEMS MFCs (D6.1),
1295 <https://doi.org/10.5281/zenodo.10522305>, 2024.

1296

1297 Smith, S.L., Yamanaka, Y., Pahlow, M. and Oschlies, A., 2009. Optimal uptake kinetics: physiological
1298 acclimation explains the pattern of nitrate uptake by phytoplankton in the ocean. *Marine Ecology Progress Series*,
1299 384, pp.1-12.
1300

1301 Steele, J.H., 1962. Environmental control of photosynthesis in the sea. *Limnology and oceanography*, 7(2),
1302 pp.137-150.
1303

1304 Steele, J.H, Henderson, E.W. (1992) The role of predation in plankton models. *Journal of Plankton Research*,
1305 14(1): 157-172.
1306

1307 Steinacher, M., Joos, F., Frölicher, T. L., Bopp, L., Cadule, P., Cocco, V., Doney, S. C., Gehlen, M., Lindsay, K.,
1308 Moore, J. K., Schneider, B., and Segschneider, J.: Projected 21st century decrease in marine productivity: a multi-
1309 model analysis, *Biogeosciences*, 7, 979–1005, <https://doi.org/10.5194/bg-7-979-2010>, 2010
1310

1311 Stock, C.A., Dunne, J.P., Fan, S., Ginoux, P., John, J., Krasting, J.P., Laufkötter, C., Paulot, F. and Zadeh, N.,
1312 2020. Ocean biogeochemistry in GFDL's Earth System Model 4.1 and its response to increasing atmospheric CO₂.
1313 *Journal of Advances in Modeling Earth Systems*, 12(10), p.e2019MS002043.
1314

1315 Stock, C.A., Dunne, J.P., Luo, J.Y., Ross, A.C., Van Oostende, N., Zadeh, N., Cordero, T.J., Liu, X. and Teng,
1316 Y.C., 2025. Photoacclimation and photoadaptation sensitivity in a global ocean ecosystem model. *Journal of*
1317 *Advances in Modeling Earth Systems*, 17(6), p.e2024MS004701.
1318

1319 Stock, C.A., 2019. Comparing apples to oranges: Perspectives on satellite-based primary production estimates
1320 drawn from a global biogeochemical model, *Journal of Marine Research*, 77, (S). [https://elischolar.library.yale-](https://elischolar.library.yale.edu/journal_of_marine_research/480)
1321 [.edu/journal_of_marine_research/480](https://elischolar.library.yale.edu/journal_of_marine_research/480).
1322

1323 Tagliabue A, Kwiatkowski L, Bopp L, Butenschön M, Cheung W, Lengaigne M and Vialard J (2021) Persistent
1324 Uncertainties in Ocean Net Primary Production Climate Change Projections at Regional Scales Raise Challenges
1325 for Assessing Impacts on Ecosystem Services. *Front. Clim.* 3:738224. doi: 10.3389/fclim.2021.738224
1326

1327 Tao, Zui & Wang, Yan & Ma, Sheng & Lv, Tingting & Zhou, Xiang. (2017). A Phytoplankton Class-Specific
1328 Marine Primary Productivity Model Using MODIS Data. *IEEE Journal of Selected Topics in Applied Earth*
1329 *Observations and Remote Sensing*. PP. 1-10. 10.1109/JSTARS.2017.2747770.
1330

1331 Tjiputra, J.F., Polzin, D. and Winguth, A.M., 2007. Assimilation of seasonal chlorophyll and nutrient data into an
1332 adjoint three-dimensional ocean carbon cycle model: Sensitivity analysis and ecosystem parameter
1333 optimization. *Global biogeochemical cycles*, 21(1).
1334

1335 Tjiputra, J.F., Couespel, D. and Sanders, R., 2025. Marine ecosystem role in setting up preindustrial and future
1336 climate. *Nature Communications*, 16(1), p.2206.

1337

1338 Thomas, M.K., Kremer, C.T. and Litchman, E. (2016), Phytoplankton temperature trait biogeography. *Global*
1339 *Ecology and Biogeography*, 25: 75-86. <https://doi.org/10.1111/geb.12387>

1340

1341 Uitz J, Claustre H, Gentili B, Stramski D. (2010). Phytoplankton class-specific primary production in the world's
1342 oceans: Seasonal and interannual variability from satellite observations. *Global Biogeochemical Cycles* 24.
1343 <https://doi.org/10.1029/2009GB003680>

1344

1345 Vichi, M., Pinardi, N. and Masina, S., 2007. A generalized model of pelagic biogeochemistry for the global ocean
1346 ecosystem. Part I: Theory. *Journal of Marine Systems*, 64(1-4), pp.89-109.

1347

1348 Ward, B.A., Dutkiewicz, S., Jahn, O. and Follows, M.J., 2012. A size-structured food-web model for the global
1349 ocean. *Limnology and Oceanography*, 57(6), pp.1877-1891.

1350

1351 Webb, W.L., Newton, M. and Starr, D., 1974. Carbon dioxide exchange of *Alnus rubra*: a mathematical model.
1352 *Oecologia*, 17, pp.281-291

1353

1354 Westberry, T., Behrenfeld, M.J., Siegel, D.A. and Boss, E., 2008. Carbon-based primary productivity modeling
1355 with vertically resolved photoacclimation. *Global Biogeochemical Cycles*, 22(2).

1356

1357 Wu, Z., S. Dutkiewicz., O. Jahn, D. Sher, A. White, and M.J. Follows, 2021. Modeling photosynthesis and
1358 exudation in the subtropical oceans. *Global Biogeochemical Cycles*, 35, doi:10.1029/2021GB006941

1359

1360 Xiao, Y. and Friedrichs, M.A., 2014. Using biogeochemical data assimilation to assess the relative skill of multiple
1361 ecosystem models in the Mid-Atlantic Bight: effects of increasing the complexity of the planktonic food web.
1362 *Biogeosciences*, 11(11), pp.3015-3030.

1363

1364 Yool, A., Popova, E.E. and Anderson, T.R., 2013. MEDUSA-2.0: an intermediate complexity biogeochemical
1365 model of the marine carbon cycle for climate change and ocean acidification studies. *Geoscientific Model*
1366 *Development*, 6(5), pp.1767-1811.

1367

1368 Young, I. R., & Ribal, A. (2019). Multiplatform evaluation of global trends in wind speed and wave height.
1369 *Science*, 364(6440), 548–552. <https://doi.org/10.1126/science.aav9527>

1370

1371 Yumruktepe, V.Ç., Samuelsen, A. and Daewel, U., 2022. ECOSMO II (CHL): a marine biogeochemical model
1372 for the North Atlantic and the Arctic. *Geoscientific Model Development*, 15(9), pp.3901-3921.

1373

1374 Zheng, Q., Viljoen, J.J., Sun, X., Kovač, Ž., Sathyendranath, S. and Brewin, R.J., 2025. Simulating vertical
1375 phytoplankton dynamics in a stratified ocean using a two-layered ecosystem model. *Biogeosciences*, 22(13),
1376 pp.3253-3278.

